prepared as a 20 mg/ml solution in dimethyl sulfoxide immediately before use.

Bacterial culture

H. pylori was prepared by the same method as described previously.[28] Briefly, *H. pylori* strain ATCC43504 (American Type Culture Collection, Rockville, MD) was grown in Brucella broth (Becton Dickinson, Cockeysville, MD) containing 7% FCS, at 37°C under microaerobic conditions using an Anaero Pack Campylo (Mitsubishi Gas Chemical, Tokyo, Japan), at high humidity for 24 hr. The broth cultures of *H. pylori* were checked under a phase contrast microscope for bacterial shape and motility.

Luciferase reporter assay on transcriptional activation of NF-κB

To assess whether NF-κB is activated by *H. pylori* infection in gastric cancer cells and to determine the effects of CAPE, luciferase reporter assays were performed. AGS cells were cotransfected in a 24-well culture plate with two expression plasmids, one including a luciferase reporter gene under transcriptional control of the NF-κB element (pNF-κB-Luc; Stratagene, La Jolla, CA) and the other a transfection efficiency indicator (pGL4.74[*hRluc*/TK] Vector; Promega, Madison, WI) using the Lipofectamin 2000 (Invitrogen) transfection reagent. After 24 hr incubation, cells were challenged by infection with 1×10^6 colony-forming units (CFU)/well of *H. pylori* and immediately treated with various concentrations of CAPE (0, 10, 20, or 40 μg/ml) for 24 hr. NF-κB luciferase reporter gene assays were performed with a Dual Luciferase Reporter Assay System (Promega) and a luminometer (Lumat LB9501; Berthold, Bad Wildbad, Germany) according to the manufacturer's instructions.

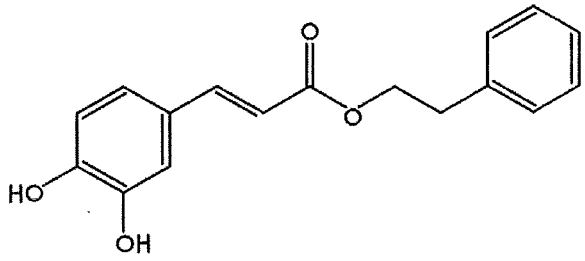

FIGURE 1 – Chemical structure of caffeic acid phenethyl ester. $C_{17}H_{16}O_4$, molecular weight 284.3.

Analysis of mRNA expression for inflammatory factors by relative quantitative real-time RT-PCR

To investigate the effects of CAPE on cytokine expression of *H. pylori*-stimulated AGS cells, real-time RT-PCR analysis was performed. AGS cells were challenged by infection with 1×10^7 colony-forming units (CFU)/dish of *H. pylori* and immediately treated with CAPE (0, 5, 10 or 20 μg/ml). After 24 hr incubation, total RNA was extracted from these cells using an RNeasy Plus Mini Kit (Qiagen, Hilden, Germany). After DNase treatment, first strand cDNAs were synthesized using a SuperScript III First-Strand Synthesis System (Invitrogen) according to the manufacturer's instructions. Relative quantitative PCR of tumor necrosis factor-α (TNF-α), interleukin (IL)-1β, IL-8, IL-10, inducible nitric oxide synthase (iNOS) and cyclooxygenase-2 (COX-2) was carried out using a LightCycler system (Roche Diagnostics, Mannheim, Germany) with the glyceraldehyde-3-phosphate dehydrogenase (GAPDH) gene as an internal control. The PCR was performed basically as described earlier using a QuantiTect SYBR Green PCR Kit (Qiagen).[29] The primer sequences for each marker are listed in Table I. Specificity of the PCR reaction was confirmed using the melting program provided with the LightCycler software. To further confirm that there was no obvious primer dimer formation or amplification of any extra bands, the samples were electrophoresed in 3% agarose gels and visualized with ethidium bromide after the LightCycler reaction. Relative quantifica-

TABLE I – PRIMER SEQUENCES FOR RELATIVE QUANTITATIVE REAL-TIME RT-PCR

Species	Gene	Sequences	Product length (bp)	Accession no.
Gerbil	GAPDH	5′-AACGGCACAGTCAAGGCTGAGAACG-3′ 5′-CAACATACTCGGCACCGGCATCG-3′	118	AB040445
	TNF-α	5′-GCCCCCACCTCGTGCTCCTCAC-3′ 5′-GGCAGGGGCTCTTGATGGCAGACAG-3′	96	AB177841
	IFN-γ	5′-AGAGCATAAACGCCATCAGG-3′ 5′-TGCTCTGGATCTGTGGATCA-3′	120	L37782
	IL-2	5′-AGCTCCTGAGAGGGATCAAC-3′ 5′-ACATCATGCAGAGGTCCAAG-3′	139	X68779
	IL-6	5′-ATGGCTGAAGTCCAAGACC-3′ 5′-GGAATGTCCTCAGCTTGGTA-3′	125	AB164706
	IL-10	5′-CAGGGCTCCTGAAAGAGTTA-3′ 5′-AGAATGAGGTCAGGGGAATC-3′	114	L37781
	iNOS	5′-GCTTGAGCGAGGAGCAGGTTGAGGA-3′ 5′-CGCTGGCCTTTTTCACCCCATAGGA-3′	111	AB177843
	KC	5′-CACCCGCTCGCTTCTTC-3′ 5′-ATGCTCTTGGGGTGAATCC-3′	138	AJ877921
Human	GAPDH	5′-GGGAAGCTTGTCATCAATGG-3′ 5′-TGGACTCCACGACGTACTCA-3′	103	NM_002046
	TNF-α	5′-AGCCCATGTTGTAGCAAACC-3′ 5′-ATGAGGTACAGGCCCTCTGA-3′	135	AF043342
	IL-1β	5′-AGGGACAGGATATGGAGCAA-3′ 5′-TTCAACACGCAGGACAGGTA-3′	127	NM_000576
	IL-8	5′-CGGAAGGAACCATCTCACTG-3′ 5′-AGCACTCCTTGGCAAAACTG-3′	116	NM_000584
	IL-10	5′-CCAAGACCCAGACATCAAGG-3′ 5′-GGCCTTGCTCTTGTTTTCAC-3′	115	NM_000572
	iNOS	5′-CCCAAGCTCTACACCTCCAA-3′ 5′-TTTGAGCCTCATGGTGAACA-3′	132	AB022318
	COX-2	5′-CGCTTTATGCTGAAGCCCTA-3′ 5′-TTTCTACCAGAAGGGCAGGA-3′	127	M90100

GAPDH, glyceraldehyde-3-phosphate dehydrogenase; TNF, tumor necrosis factor; IFN, interferon; IL, interleukin; iNOS, inducible nitric oxide synthase; COX, cyclooxygenase.

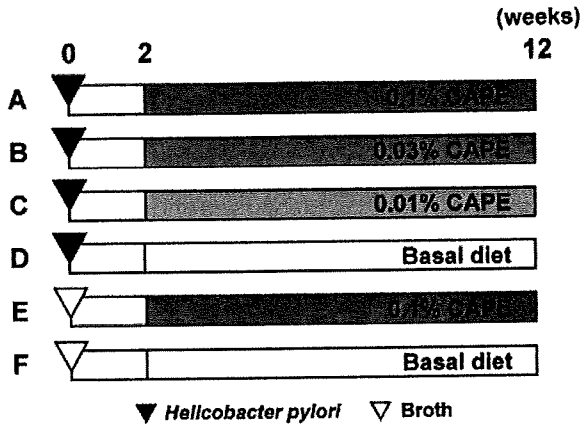

FIGURE 2 – Experimental design. Six-week-old male Mongolian gerbils were inoculated with *Helicobacter pylori* (ATCC43504 strain) or Brucella broth. After 2 weeks, animals were given basal diets (CE-2) containing caffeic acid phenethyl ester (CAPE) at various concentrations (0, 0.01, 0.03 and 0.1%) for 10 weeks.

tion was performed as previously established using the internal control without the necessity for external standards.[29]

Western blot analysis

Total protein extract was obtained from *H. pylori*-stimulated and CAPE-treated AGS cells by a Nuclear Extract Kit (Active Motif, Carlsbad, CA). Protein samples were fractionated by SDS-PAGE and electrophoretically transferred to a PVDF membrane. Blots were blocked with 5% nonfat dry milk in tris-buffered saline for 1 hr and then incubated over night with a rabbit polyclonal anti-IκB-α antibody (Cell Signaling Technology, Beverly, MA), a mouse monoclonal anti-α-tubulin antibody (clone DM1A, Santa Cruz Biotechnology, Santa Cruz, CA), a rabbit polyclonal anti-phospho-NF-κB p65 antibody (Ser276, Cell Signaling Technology) and a mouse monoclonal anti-actin antibody (clone ACTN05, Thermo Scientific, Fremont, CA). Detection was performed using an Immun-Star HRP Chemiluminescent Kit (Bio-Rad Laboratories, Hercules, CA).

In vivo *experimental design*

The experimental design is illustrated in Figure 2. A total of 55 specific pathogen-free male, 6-week-old Mongolian gerbils (*Meriones unguiculatus*; MGS/Sea, Kyudo, Fukuoka, Japan) were used. They were housed in plastic cages on hardwood-chip bedding in an air-conditioned biohazard room with a 12-hr light/12-hr dark cycle, and allowed free access to food and water throughout. The gerbils were divided into 6 groups (Groups A–F). Animals of Groups A–D were inoculated with 1.0 ml of broth culture containing *H. pylori* (1×10^8 CFU/ml) intragastrically using an oral catheter, while gerbils of Groups E and F were inoculated with Brucella broth alone. From weeks 2 to 12, the gerbils received CE-2 diets (CLEA Japan, Tokyo, Japan) containing CAPE at the concentrations of 0.1% (Groups A and E), 0.03% (Group B), 0.01% (Group C) and 0% (Groups D and F). All experimental diets were prepared at 8 day intervals in our laboratory and stored in a refrigerator. Food cups were replenished with fresh diet every second day. At week 12, all gerbils were intraperitoneally injected with 5′-bromo-2′-deoxyuridine (BrdU) at a dose of 100 mg/kg, 1 hr before sacrifice. The animals were then subjected to deep anesthesia and laparotomy with excision of the stomach, liver, spleen, kidney, heart and lung, and blood samples were collected from the inferior vena cava. The experimental design was approved by the Animal Care Committee of the Aichi Cancer Center Research Institute, and the animals were cared for in accordance with institutional guidelines as well as the Guidelines for Proper Conduct of Animal Experiments (Science Council of Japan, June 1, 2006).

Histopathology and immunohistochemistry

The excised stomachs were fixed in 10% neutral-buffered formalin for 24 hr and sliced along the longitudinal axis into 4–8 strips of equal width, and embedded in paraffin. Serial paraffin sections were prepared and stained with hematoxylin and eosin (H&E) for morphological observation. The glandular mucosa of the antrum and corpus was examined histologically for inflammation and epithelial changes. The degree of chronic active gastritis was graded according to criteria modified from the Updated Sydney System,[30] by scoring the infiltration of neutrophils and mononuclear cells, intestinal metaplasia and heterotopic proliferative glands, on a four-point scale (0–3; 0, normal; 1, mild; 2, moderate; 3, marked). Epithelial cell proliferation was assessed by BrdU labeling, visualized by immunostaining with a mouse monoclonal anti-BrdU antibody (clone Bu20a, diluted 1:1000, Dako, Glostrup, Denmark) as described previously.[31] Labeling indices in BrdU-stained slides were determined as the mean percentages of BrdU-positive epithelial cells among total cells in 10 different randomly selected glands in both the antrum and corpus. Immunohistochemical analyses were carried out with a mouse monoclonal anti-COX-2 antibody (clone 33, diluted 1:100, BD Biosciences, San Jose, CA), a mouse monoclonal anti-phospho-IκB-α antibody (clone 5A5, diluted 1:150, Cell Signaling Technology) and a rabbit polyclonal anti-NFκB p50 antibody (clone H-119, diluted 1:100, Santa Cruz Biotechnology) as previously described.[32–34] To quantitate the degree of staining, a grading system was employed with the following criteria: grade 0 (negative), grades 1–3 (increasing degrees of intermediate immunoreactivity) and grade 4 (extensive reactivity).

Gland isolation

Gland isolation was performed as previously described.[35] Briefly, remaining portions of resected gastric mucosa were injected with calcium- and magnesium-free Hanks' balanced salt solution (HBSS) containing 30 mM ethylenediaminetetraacetic acid (EDTA) submucosally, incubated in EDTA-HBSS, and shaken for 15 min at 37°C. Then the mucosa was scraped off with a scalpel. Isolated glands were washed in phosphate buffered saline, fixed in 70% ethanol for a few hours, dehydrated with 95% ethanol, and stored at −20°C until use.

Analysis of mRNA expression in the pyloric mucosa of Mongolian gerbils

Relative quantitative real-time RT-PCR for TNF-α, interferon-γ (IFN-γ), IL-2, IL-6, IL-10, iNOS and IL-8 homologue (KC) was carried out using total RNA extracted from selected pyloric mucosal tissue with the gerbil-specific GAPDH gene as an internal control same as above. The expression levels of mRNAs were expressed relative to 1.0 in the control group (Group F).

Serology

Blood samples were centrifuged and separated sera were stored at −80°C until use. The titer of anti-*H. pylori* antibodies was measured using an ELISA kit (Biomerica, Newport Beach, CA) and values were expressed using an arbitrary index (AI).[27] Sera were also used for measurement of gastrin levels (SRL, Tokyo, Japan).

Statistical analysis

Quantitative values were expressed as means ± SD or SE, and differences between means were statistically analyzed by ANOVA or Kruskal-Wallis followed by a multiple comparison test. p values of less than 0.05 were considered to be statistically significant.

Results

Suppressive effects of CAPE on H. pylori*-induced NF-κB activation and mRNA expression of inflammatory factors in AGS cells*

NF-κB activation in *H. pylori*-stimulated AGS cells was significantly increased as compared to that in noninfected control cells ($p < 0.01$) (Fig. 3). CAPE decreased the *H. pylori*-induced NF-κB transcriptional activation in a dose-dependent manner, with significance at the 20 and 40 μg/ml doses ($p < 0.05$ and $p < 0.01$, respectively). Relative quantitative real time RT-PCR data for mRNA expression of inflammatory cytokines and enzymes in the AGS cells are summarized in Figure 4. IL-8 mRNA expression in 20 μg/ml CAPE-treated cells was significantly suppressed as compared to *H. pylori*-stimulated control cells. Levels of TNF-α mRNA in 20 and 10 μg/ml CAPE-treated cells and IL-1β and iNOS mRNAs in all CAPE-treated cells were also markedly lower than in positive control. There were no significant differences in IL-10 and COX-2 expression among *H. pylori*-infected cells.

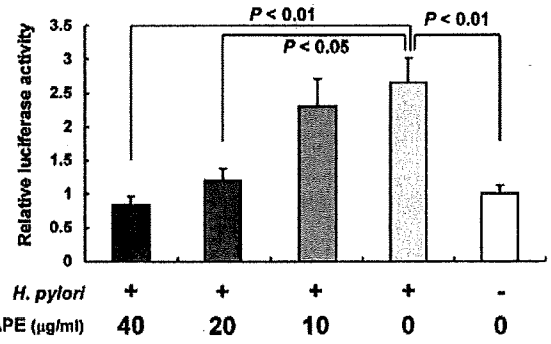

FIGURE 3 – Luciferase reporter assay for transcriptional activation of nuclear factor-κB (NF-κB) in the AGS gastric cancer cell line. Elevated transcriptional activation of NF-κB was induced after infection with *Helicobacter pylori* (*H. pylori*). Note the dose-dependent inhibition of NF-κB activation by caffeic acid phenethyl ester (CAPE) treatment compared with the vehicle control (0.1% dimethyl sulfoxide). Values are means ± SDs of data from three independent experiments.

CAPE prevents IκB-α degradation and phosphorylation of NF-κB p65 in AGS cells

We assessed the degradation of IκB-α and phosphorylation of p65 subunit by Western blot analysis (Fig. 5). Western blotting showed that *H. pylori* stimulation up-regulated the phosphorylation of p65 and IκB-α degradation in AGS cells. CAPE treatment inhibited the phosphorylation of p65 and degradation of IκB-α in a dose-dependent manner.

Average body weights, relative organ weights and serological results

Data for average body weights, titers of anti-*H. pylori* antibodies, serum gastrin levels and relative organ weights are summarized in Table II. The average body weight in the 0.1% CAPE-treated and *H. pylori*-infected group (Group A) was significantly higher than for the other *H. pylori*-infected groups (Groups B–D) ($p < 0.01$). AI values for anti-*H. pylori* antibody titers and serum gastrin levels were markedly up-regulated by *H. pylori* infection ($p < 0.01$ and $p < 0.05$, respectively). There were no significant differences in the relative organ weights of liver and kidney between 0.1% CAPE-treated and noninfected gerbils (Group E) and untreated controls (Group F). The relative kidney weights in the *H. pylori*-infected group (Group D) were markedly higher than in Group F ($p < 0.05$). No macroscopic or microscopic lesions

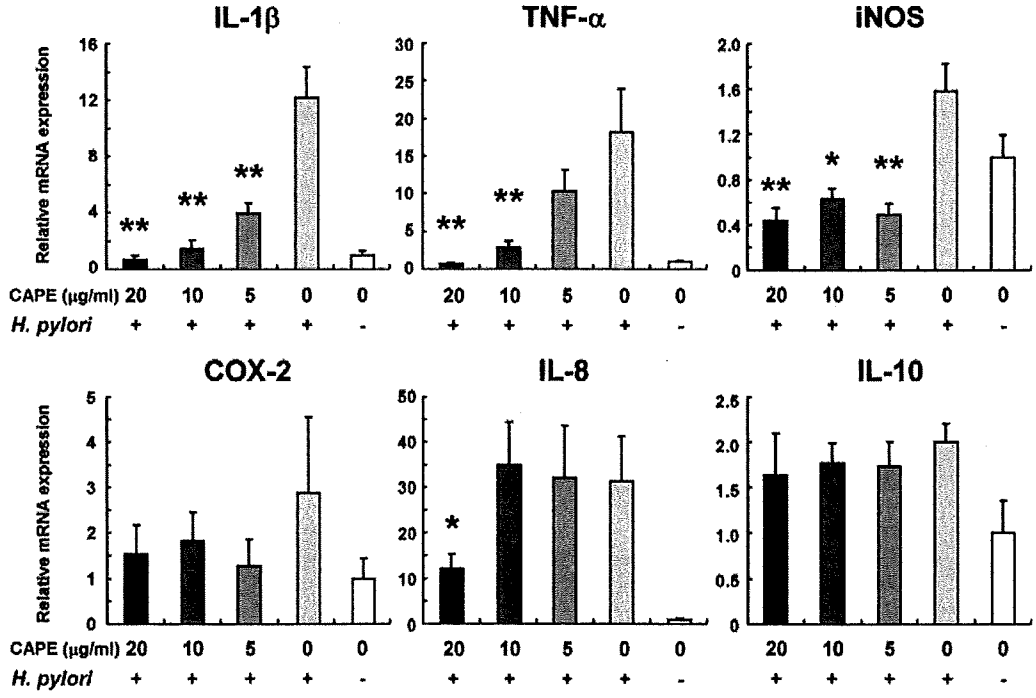

FIGURE 4 – Relative expression levels of interleukin (IL)-1β, tumor necrosis factor-α (TNF-α), inducible nitric oxide synthase (iNOS), cyclooxygenase-2 (COX-2), IL-8 and IL-10 mRNAs in the AGS gastric cancer cell line. Values were set at 1.0 in untreated control and expressed as mean ± SE relative values. Note that the *Y*-axes have different scales. *$p < 0.05$ and **$p < 0.01$ *vs. H. pylori*-infected and CAPE-untreated samples.

were observed in nonstomach internal organs, including the liver, spleen, kidney, heart and lung of all groups.

Inhibitory effects of CAPE on H. pylori*-induced gastritis*

The gastric mucosa of *H. pylori*-infected groups (Groups A–D) was generally thickened and edematous, with occasional erosions and ulceration. Such macroscopic lesions were not recognized in the stomachs of noninfected gerbils, and gastric mucosal specimens from these gerbils had normal histomorphology. Histological findings for chronic gastritis in each group are summarized in Table III. Infiltration of neutrophils in both the antrum and corpus and of mononuclear cells in the antrum of Group A animals (*H. pylori* + 0.1% CAPE) was significantly suppressed as compared to Group D ($p < 0.05$ and 0.01, respectively) (Figs. 6*a*, 6*e*, and 6*i*). There were no significant differences in scores for intestinal metaplasia, heterotopic proliferative glands and COX-2 immunoreactivity among Groups A–D. Macroscopic and microscopic analyses revealed no significant differences between gerbils in Groups E and F, so Group E was excluded from subsequent analyses of BrdU labeling indices, immunohistochemistry of NF-κB p50 and phospho-IκB-α and transcriptional expression of inflammatory factors. Immunohistochemistry of NF-κB p50 and phospho-IκB-α revealed that strong reactivity of gastric epithelium and infiltrated cells in *H. pylori*-infected gerbils, and CAPE treatment significantly reduced the immunohistochemical scores (Figs. 6*c*, 6*d*, 6*g*, 6*h*, 6*k*, and 6*l*).

BrdU labeling indices in gastric epithelial cells

In *H. pylori*-infected gerbils, BrdU-labeled epithelial nuclei were found distributed throughout the hyperplastic mucosa, while BrdU-positive cells in noninfected animals were located in the neck portions of glands (Figs. 6*b*, 6*f*, and 6*j*). At 12 weeks, BrdU labeling indices in both the antrum and corpus of Group A (*H. pylori* + 0.1% CAPE) were significantly suppressed as compared to Group D ($p < 0.01$; Fig. 7). Similarly, BrdU labeling indices in the antrum of the 0.03% CAPE-treated group (Group B) were significantly lowered ($p < 0.05$), without significant decrease in the corpus.

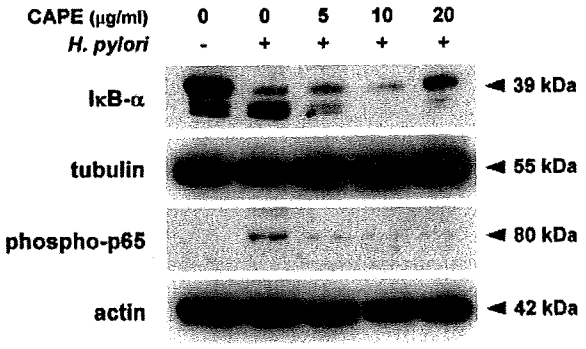

FIGURE 5 – Western blotting for IκB-α and phospho-p65 in AGS cells. CAPE prevents IκB-α degradation and p65 phosphorylation in a dose-dependent manner. A representative data of three independent experiments is shown.

Hyperplasia in isolated pyloric glands

To evaluate the effect of CAPE on *H. pylori*-induced mucosal hyperplasia, we analyzed the length of isolated glands from the pyloric mucosa (Fig. 8*a*). The average value for Group A (*H. pylori* + 0.1% CAPE) was significantly reduced compared to that for Group D ($p < 0.05$) (Fig. 8*b*).

Expression of inflammatory factors in the pyloric mucosa

RT-PCR data for mRNA expression of inflammatory cytokines and enzymes in the pyloric mucosa of gerbils are summarized in Figure 9. TNF-α and iNOS mRNA expression in Group A (*H. pylori* + 0.1% CAPE) was significantly suppressed as compared to Group D ($p < 0.05$). Levels of IL-2 mRNA in Groups A and B and IFN-γ and IL-6 mRNAs in all CAPE-treated groups (Groups A–C) were also markedly lower than in Group D ($p < 0.05$). Only very low mRNA expression was evident in Group F.

Discussion

In this study, we demonstrated that NF-κB transcriptional activation in *H. pylori*-stimulated AGS gastric cancer cells were significantly inhibited by CAPE treatment in a dose-dependent manner. This result is consistent with a previous report that CAPE inhibits *H. pylori*-induced DNA-binding activity of NF-κB in gastric cancer cells.[9] We found that CAPE treatment resulted in a decrease of the phosphorylation of NF-κB p65 subunit and inhibition of IκB-α degradation. In addition, relative quantitative real-time RT-PCR analysis revealed that mRNA expressions of several inflammatory factors including IL-1β, TNF-α, iNOS, and IL-8 in NF-κB-activated AGS cells were significantly suppressed by CAPE treatment in a dose-dependent manner, whereas there were no statistical differences in COX-2 and IL-10 expression. IκB-α degradation induces the phosphorylation of p65 and following nuclear transition of NF-κB complex. Thus, our data suggested that CAPE may prevent *H. pylori*-induced NF-κB activation and transcriptional activity of inflammatory factors through the inhibition of nuclear translocation of NF-κB.

Here we found that oral administration of CAPE effectively inhibited gastric inflammation at 0.1% in the diet with significant suppression of infiltration of neutrophils both in the antrum and corpus and mononuclear cells in the antrum at week 12. Fitzpatrick *et al.* earlier reported CAPE to inhibit TNF-α production in a rat macrophage cell line and TNF-α-stimulated IL-8 production in human colonic epithelial cells.[36] Expression of IL-8, a potent chemokine stimulus for neutrophil migration, is increased with *H. pylori* infection through NF-κB activation.[17] In this study, mRNA expression of TNF-α and IL-8 in *H. pylori*-stimulated AGS cells were significantly decreased by CAPE treatment. Similarly, CAPE markedly suppressed the expression of TNF-α and KC protein, one of the IL-8 homologues, in *H. pylori*-infected gerbils. The

TABLE II – SUMMARY OF THE ANIMAL EXPERIMENT

Group	Treatment	Effective number	Body weight (g)	Anti-*Hp* IgG titer (AI)	Serum gastrin (pg/ml)	Relative organ weights (%)	
						Liver	Kidney
A	*Hp* + 0.1% CAPE	10	81.4 ± 8.7[1]	8.4 ± 3.1[2]	187 ± 52.3[3]	3.88 ± 0.25	0.82 ± 0.07
B	*Hp* + 0.03% CAPE	10	73.5 ± 4.8	11.5 ± 4.2[2]	176 ± 35.3[3]	3.74 ± 0.17	0.82 ± 0.04
C	*Hp* + 0.01% CAPE	10	72.6 ± 4.2	15.9 ± 7.3[2]	192 ± 93.2[3]	3.66 ± 0.27	0.80 ± 0.05
D	*Hp*	10	73.0 ± 6.8	10.6 ± 5.4[2]	185 ± 45.8[3]	3.74 ± 0.13	0.83 ± 0.06[3]
E	Broth + 0.1% CAPE	5	69.5 ± 4.9	0.7 ± 0.4	126 ± 16.7	3.59 ± 0.30	0.73 ± 0.24
F	Broth	10	75.2 ± 6.4	0.5 ± 0.1	125 ± 54.8	3.75 ± 0.21	0.77 ± 0.04

Values for results are expressed as means ± SD. *Hp*, *Helicobacter pylori*; AI, arbitrary index; CAPE, caffeic acid phenethyl ester.
[1]$p < 0.01$ *vs.* Group B–D.–[2]$p < 0.01$ *vs.* Group F.–[3]$p < 0.05$ *vs.* Group F.

TABLE III – HISTOPATHOLOGICAL EVALUATION OF GASTRITIS

Group	Treatment	Effective number	Infiltration of neutrophils		Infiltration of mononuclear cells		Intestinal metaplasia		Heterotopic proliferative glands		Score of COX-2 immunohistochemistry	
			Antrum	Corpus	Antrum	Corpus	Antrum	Corpus	Antrum	Corpus	Antrum	Corpus
A	*Hp* + 0.1% CAPE	10	1.8 ± 0.4[1]	1.1 ± 0.6[1]	2.3 ± 0.3[2]	1.6 ± 0.4	0.0 ± 0.0	0.0 ± 0.0	1.1 ± 0.4	0.6 ± 0.4	1.3 ± 0.5	0.9 ± 0.7
B	*Hp* + 0.03% CAPE	10	2.6 ± 0.5	2.1 ± 0.8	2.9 ± 0.2	2.3 ± 0.5	0.1 ± 0.3	0.2 ± 0.4	1.3 ± 0.5	1.0 ± 0.7	1.6 ± 0.5	1.3 ± 0.8
C	*Hp* + 0.01% CAPE	10	2.1 ± 0.4	2.0 ± 0.9	2.6 ± 0.5	2.2 ± 0.6	0.1 ± 0.3	0.1 ± 0.3	1.1 ± 0.4	0.9 ± 0.4	1.4 ± 0.5	0.9 ± 0.6
D	*Hp*	10	2.5 ± 0.5	2.2 ± 0.7	2.9 ± 0.2	2.2 ± 0.6	0.1 ± 0.3	0.1 ± 0.3	1.1 ± 0.5	0.9 ± 0.7	1.7 ± 0.7	1.2 ± 0.8
E	Broth + 0.1% CAPE	5	0.0 ± 0.0	0.1 ± 0.2	0.0 ± 0.0	0.0 ± 0.0	0.0 ± 0.0	0.0 ± 0.0	0.0 ± 0.0	0.0 ± 0.0	0.2 ± 0.4	0.2 ± 0.4
F	Broth	10	0.1 ± 0.2	0.0 ± 0.0	0.2 ± 0.2	0.0 ± 0.0	0.0 ± 0.0	0.0 ± 0.0	0.0 ± 0.0	0.0 ± 0.0	0.1 ± 0.3	0.0 ± 0.0

Values for results are expressed as means ± SD. COX-2, cyclooxygenase-2; *Hp*, *Helicobacter pylori*; CAPE, caffeic acid phenethyl ester.
[1] $p < 0.05$ *vs.* Group D. [2] $p < 0.01$ *vs.* Group D.

inhibitory effects of CAPE on infiltration of neutrophils observed in this study may therefore be explained by reduction of NF-κB-associated cytokines, including TNF-α and KC.

Phosphorylation of IκB-α acts as a trigger of IκB degradation, allowing the nuclear translocation of NF-κB complex and activation of gene expression. In our study, 0.1% CAPE-containing diet inhibited the immunohistochemical expression of phosphorylated IκB-α and nuclear transition of NF-κB p50 subunit in the gastric mucosa of *H. pylori*-infected gerbils, suggesting that CAPE has chemopreventive potentials by inhibiting the NF-κB pathway.

Our findings for BrdU-labeled cells in the gastric mucosa and average lengths of isolated pyloric glands suggest that *H. pylori*-induced chronic gastritis and epithelial hyper-proliferation are efficiently suppressed by CAPE administration. Previous clinical studies have demonstrated that epithelial proliferation is positively correlated with the degree of histological inflammation in the gastric mucosa of *H. pylori*-infected patients.[37] We have previously reported that the severity of gastritis plays an important role in *H. pylori*-associated gastric carcinogenesis in gerbils, with essential involvement of chronic inflammation and increased rates of cell proliferation.[38] Therefore, it is very conceivable that CAPE might reduce gastric carcinogenesis as well as chronic gastritis.

Our demonstration that mRNA expression levels of inflammatory factors including TNF-α, IFN-γ, IL-2, IL-6, iNOS and KC were significantly decreased by CAPE treatment in the pyloric mucosa of *H. pylori*-infected Mongolian gerbils is of clear interest. All these factors are known to be induced by NF-κB transcriptional activation.[5,39] It has been reported that a predominant *H. pylori*-specific Th1 response characterized by TNF-α and IFN-γ production is associated with *H. pylori*-infected gastritis.[40] Several studies have demonstrated that IFN-γ and IL-6 play important roles in progression of pyloric gastritis in *H. pylori*-infected gerbils.[20,33] In addition, TNF-α is a mediator during inflammation and tumor promotion, leading to activation of NF-κB and thereby suppression of cell death and stimulation of cell proliferation.[41] Interestingly, although significant suppressive effects of CAPE on IL-6 and IFN-γ expression in the antrum were observed in all CAPE-treated groups, gastritis was attenuated only in 0.1% CAPE-treated gerbils. Thus, our results suggest that TNF-α and iNOS might be key molecules, in addition to other factors, suppressing *H. pylori*-induced chronic gastritis in Mongolian gerbils. iNOS is also known to be up-regulated by *H. pylori* and to enhance progression of gastric inflammation and carcinogenesis through generation of reactive oxygen species.[42]

On the other hand, expression level of COX-2 was not suppressed by CAPE treatment both in *H. pylori*-stimulated AGS cells and in the pyloric mucosa of gerbils. Several studies demonstrated that gastric COX-2 expression in *H. pylori*-infected humans and rodents could be associated with repair of mucosal injury.[43–45] Thus, there is a possibility that COX-2 expression may play important roles both in mediation of gastritis and in healing of *H. pylori*-associated gastric ulceration. CAPE treatment also showed no effects on mRNA expression of IL-10 in AGS cells and the pyloric mucosa of gerbils. IL-10 has been known as an anti-inflammatory cytokine, and demonstrated to inhibit other inflammatory cytokines and chemokines in *H. pylori*-induced gastritis.[46,47] Our result of stable expression of IL-10 may reflect an increase of anti-inflammatory cytokine activity through the separate cascade from NF-κB pathway.

CAPE concentrations in the range of 0.01–0.1% were chosen for the present investigation because a previous study in mice demonstrated no toxicity at 0.15% CAPE given for 110 days.[11] In this study, there were no significant differences in relative organ weights of liver and kidney between 0.1% CAPE-treated (Group E) and nontreated gerbils (Group F). In addition, no macroscopic and microscopic lesions were observed in the non-gastric internal organs, including liver, spleen, kidney, heart and lung of CAPE-treated gerbils. Therefore, we conclude that the

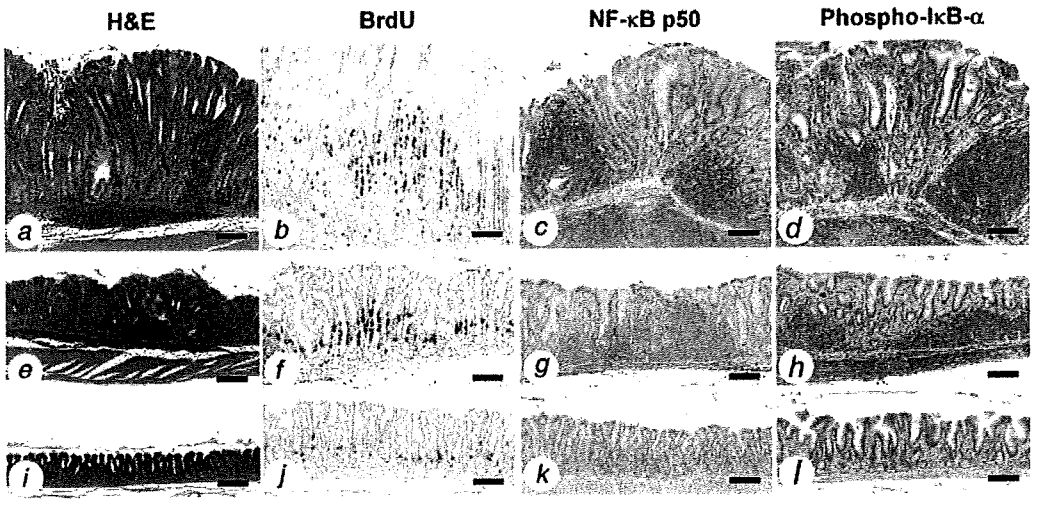

FIGURE 6 – Histopathology and immunohistochemistry findings for the gastric mucosa of Mongolian gerbils. *Helicobacter pylori* (*H. pylori*) + basal diet group (Group D, panels *a–d*), *H. pylori* + 0.1% caffeic acid phenethyl ester (CAPE) group (Group A, panels *e–h*) and Broth + basal diet group (Group F, panels *i–l*). (*a*) Marked mucosal hyperplasia with severe infiltration of neutrophils and mononuclear cells (H&E, ×50, Bar = 200 μm). (*b*) Large numbers of BrdU-positive cells are apparent in hyperplastic mucosal epithelium (BrdU immunostaining, ×100, Bar = 100 μm). (*c* and *d*) Strong expression of NF-κB p50 and phospho-IκB-α is observed in gastric epithelium and infiltrated cells (NF-κB p50 and phospho-IκB-α immunostaining, respectively, ×100, Bar = 100 μm). (*e*) Mild to moderate gastritis (H&E, ×50, Bar = 200 μm). (*f*) Note moderate numbers of BrdU-positive cells (BrdU, ×100, Bar = 100 μm). (*g* and *h*) Relatively weak expression of NF-κB p50 and phospho-IκB-α in 0.1% CAPE-treated gerbils (NF-κB p50 and phospho-IκB-α, ×100, Bar = 100 μm). (*i*) No lesions are observed in the gastric mucosa of a noninfected gerbil (H&E, ×50, Bar = 200 μm). (*j*) BrdU-positive cells are present only in the proliferative zone of a noninfected animal (BrdU, ×100, Bar = 100 μm). (*k* and *l*) NF-κB p50 and phospho-IκB-α expression is weak in a noninfected gerbil (NF-κB p50 and phospho-IκB-α, ×100, Bar = 100 μm).

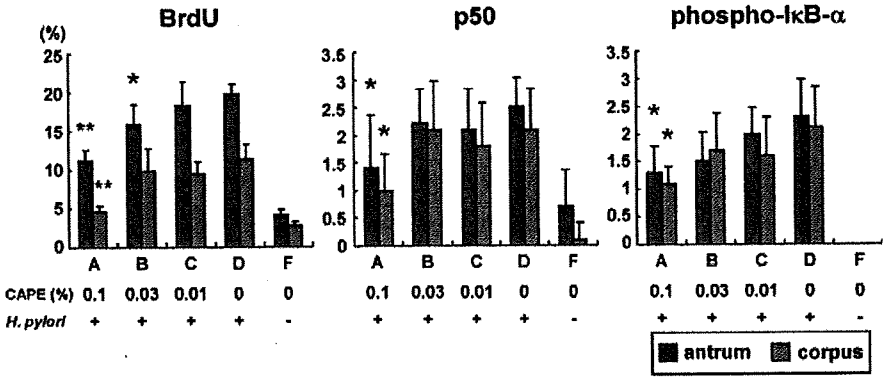

FIGURE 7 – Immunohistochemical analysis of BrdU, NF-κB p50, and phospho-IκB-α staining in the antrum and corpus of Mongolian gerbils. BrdU staining was evaluated by mean percentages of BrdU-positive cells among total cells in 10 selected glands, and NF-κB p50 and phospho-IκB-α staining were scored 0–4. Data are presented as mean ± SD values. $*p < 0.05$ and $**p < 0.01$ *vs.* Group D.

toxicity of CAPE is negligible at the doses used in the present study. Our data showed that relative kidney weight of *H. pylori*-infected group (Group D) was statistically higher than that of Group F. Several authors have discussed whether *H. pylori* infection is associated with the pathogenesis of renal failures in humans, but the relationship is still unclear.[48,49] Because there were no macroscopic and microscopic renal lesions in the gerbils, more detail examination is needed to clarify the association of renal weight change and *H. pylori* infection. Regarding body weight, 0.1% CAPE-treated and *H. pylori*-infected gerbils (Group A) were heavier than those in other infected groups (Groups B–D). However, animals in Group E showed no significant increase. Since there were no marked differences in serum total cholesterol and triglyceride levels between Groups A and D (data not shown), there may not be significant relevance between CAPE ingestion and body weight change.

In conclusion, our study clearly demonstrated: (1) CAPE treatment inhibits *H. pylori*-induced NF-κB activation by suppression of IκB-α degradation and phosphorylation of p65 in a gastric cancer cell line, and (2) CAPE exerts anti-inflammatory effects on *H. pylori*-induced gastritis in Mongolian gerbils with reduction of nuclear transition of NF-κB p50 through phosphorylation of IκB-α

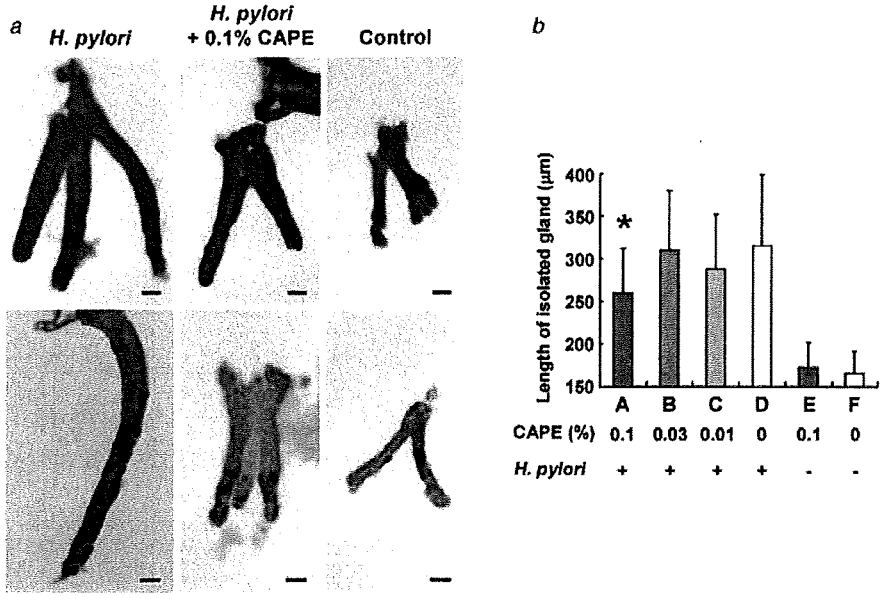

FIGURE 8 – Isolated glands from the pyloric mucosa of Mongolian gerbils. (*a*) Histopathology and immunohistochemistry of isolated pyloric glands (Upper column, H&E; Lower column, BrdU staining, ×200, Bar = 25 μm). Note the *Helicobacter pylori*-induced hyperplasia and cell proliferation activity is attenuated by 0.1% CAPE treatment. (*b*) Average lengths of isolated pyloric glands of Mongolian gerbils. Data are mean ± SD values. Note that the *Y*-axis starts from 150. $*p < 0.05$ *vs.* Group D.

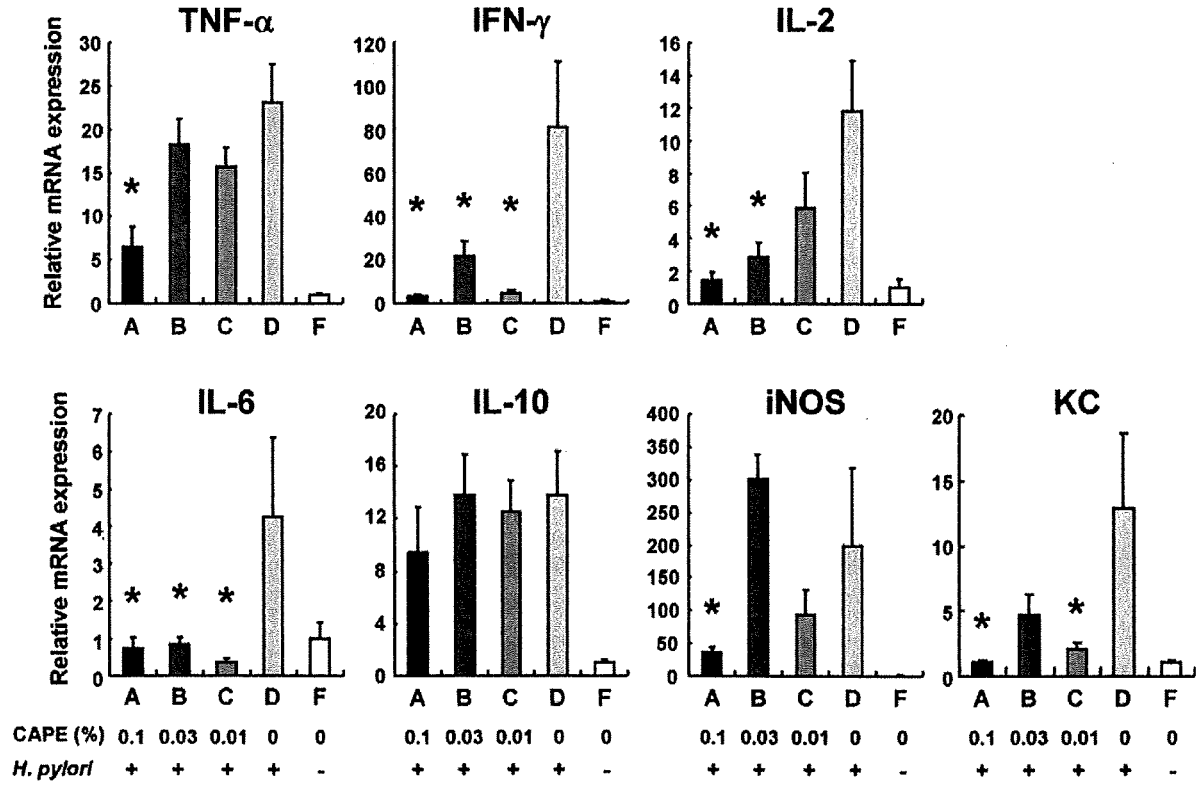

FIGURE 9 – Relative expression levels of tumor necrosis factor-α (TNF-α), interferon-γ (IFN-γ), interleukin (IL)-2, IL-6, IL-10, inducible nitric oxide synthase (iNOS), and KC mRNAs in the pyloric mucosa of Mongolian gerbils at 12 weeks postinfection. Values were set at 1.0 in Group F and expressed as mean ± SE relative values. Note that the *Y*-axes have different scales. $*p < 0.05$ *vs.* Group D.

and suppression of the mRNA expression of many NF-κB-associated inflammatory factors. These results suggest that CAPE may have potential as an alternative drug for chemoprevention of chronic active gastritis and other *H. pylori*-associated gastric disorders, including stomach adenocarcinomas.

Acknowledgements

The authors thank Ms. Noriko Saito and Ms. Ayumi Saito for their expert technical assistance.

References

1. Bonizzi G, Karin M. The two NF-κB activation pathways and their role in innate and adaptive immunity. Trends Immunol. 2004;25:280–8.
2. Coussens LM, Werb Z. Inflammation and cancer. Nature 2002;420:860–7.
3. Calzado MA, Bacher S, Schmitz ML. NF-κB inhibitors for the treatment of inflammatory diseases and cancer. Curr Med Chem 2007; 14:367–76.
4. Inoue J, Gohda J, Akiyama T, Semba K. NF-κB activation in development and progression of cancer. Cancer Sci 2007;98:268–74.
5. Umezawa K, Ariga A, Matsumoto N. Naturally occurring and synthetic inhibitors of NF-κB functions. Anticancer Drug Des 2000; 15:239–44.
6. Olivier S, Robe P, Bours V. Can NF-κB be a target for novel and efficient anti-cancer agents? Biochem Pharmacol 2006;72: 1054–68.
7. Natarajan K, Singh S, Burke TR, Jr, Grunberger D, Aggarwal BB. Caffeic acid phenethyl ester is a potent and specific inhibitor of activation of nuclear transcription factor NF-κB. Proc Natl Acad Sci USA 1996;93:9090–5.
8. Grunberger D, Banerjee R, Eisinger K, Oltz EM, Efros L, Caldwell M, Estevez V, Nakanishi K. Preferential cytotoxicity on tumor cells by caffeic acid phenethyl ester isolated from propolis. Experientia 1988;44:230–2.
9. Abdel-Latif MM, Windle HJ, Homasany BS, Sabra K, Kelleher D. Caffeic acid phenethyl ester modulates *Helicobacter pylori*-induced nuclear factor-kappa B and activator protein-1 expression in gastric epithelial cells. Br J Pharmacol 2005;146:1139–47.
10. Chen MF, Keng PC, Lin PY, Yang CT, Liao SK, Chen WC. Caffeic acid phenethyl ester decreases acute pneumonitis after irradiation *in vitro* and *in vivo*. BMC Cancer 2005;5:158–66.
11. Mahmoud NN, Carothers AM, Grunberger D, Bilinski RT, Churchill MR, Martucci C, Newmark HL, Bertagnolli MM. Plant phenolics decrease intestinal tumors in an animal model of familial adenomatous polyposis. Carcinogenesis 2000;21:921–7.
12. Carrasco-Legleu CE, Marquez-Rosado L, Fattel-Fazenda S, Arce-Popoca E, Perez-Carreon JI, Villa-Trevino S. Chemoprotective effect of caffeic acid phenethyl ester on promotion in a medium-term rat hepatocarcinogenesis assay. Int J Cancer 2004;108:488–92.
13. Uemura N, Okamoto S, Yamamoto S, Matsumura N, Yamaguchi S, Yamakido M, Taniyama K, Sasaki N, Schlemper RJ. *Helicobacter pylori* infection and the development of gastric cancer. N Engl J Med 2001;345:784–9.
14. IARC Working Group on the Evaluation of Carcinogenic Risks to Humans. Infection with *Helicobacter pylori*. In: Schistosomes, Liver Flukes and *Helicobacter pylori*, IARC Monographs on the Evaluation of Carcinogenic Risks to Humans, vol.61. Lyon, World Health Organization/International Agency for Research on Cancer, 1994.177–241.
15. Malfertheiner P, Megraud F, O'Morain C, Bazzoli F, El-Omar E, Graham D, Hunt R, Rokkas T, Vakil N, Kuipers EJ. Current concepts in the management of *Helicobacter pylori* infection: the Maastricht III Consensus Report. Gut 2007;56:772–81.
16. Gerrits MM, van Vliet AH, Kuipers EJ, Kusters JG. *Helicobacter pylori* and antimicrobial resistance: molecular mechanisms and clinical implications. Lancet Infect Dis 2006;6:699–709.
17. Keates S, Hitti YS, Upton M, Kelly CP. *Helicobacter pylori* infection activates. NF-κB in gastric epithelial cells. Gastroenterology 1997; 113:1099–109.
18. Maeda S, Yoshida H, Ogura K, Mitsuno Y, Hirata Y, Yamaji Y, Akanuma M, Shiratori Y, Omata M. *H. pylori* activates NF-κB through a signaling pathway involving IκB kinases. NF-κB-inducing kinase. TRAF2, and TRAF6 in gastric cancer cells. Gastroenterology 2000; 119:97–108.
19. Crabtree JE, Court M, Aboshkiwa MA, Jeremy AH, Dixon MF, Robinson PA. Gastric mucosal cytokine and epithelial cell responses to *Helicobacter pylori* infection in Mongolian gerbils. J Pathol 2004; 202:197–207.
20. Yamaoka Y, Yamauchi K, Ota H, Sugiyama A, Ishizone S, Graham DY, Maruta F, Murakami M, Katsuyama T. Natural history of gastric mucosal cytokine expression in *Helicobacter pylori* gastritis in Mongolian gerbils. Infect Immun 2005;73:2205–12.
21. Kim SG, Kim JS, Kim JM, Chae Jung H, Sung Song I. Inhibition of proinflammatory cytokine expression by NF-κB (p65) antisense oligonucleotide in *Helicobacter pylori*-infected mice. Helicobacter 2005; 10:559–66.
22. Ogura K, Maeda S, Nakao M, Watanabe T, Tada M, Kyutoku T, Yoshida H, Shiratori Y, Omata M. Virulence factors of *Helicobacter pylori* responsible for gastric diseases in Mongolian gerbil. J Exp Med 2000;192:1601–10.
23. Wu CS, Chen MF, Lee IL, Tung SY. Predictive role of nuclear factor-κB activity in gastric cancer: a promising adjuvant approach with caffeic acid phenethyl ester. J Clin Gastroenterol 2007;41:894–900.
24. Tatematsu M, Tsukamoto T, Inada K. Stem cells and gastric cancer: role of gastric and intestinal mixed intestinal metaplasia. Cancer Sci 2003;94:135–41.
25. Otsuka T, Tsukamoto T, Tanaka H, Inada K, Utsunomiya H, Mizoshita T, Kumagai T, Katsuyama T, Miki K, Tatematsu M. Suppressive effects of fruit-juice concentrate of *Prunus mume* Sieb. et Zucc. (Japanese apricot. Ume) on *Helicobacter pylori*-induced glandular stomach lesions in Mongolian gerbils. Asian Pac J Cancer Prev 2005;6:337–41.
26. Toyoda T, Tsukamoto T, Mizoshita T, Nishibe S, Deyama T, Takenaka Y, Hirano N, Tanaka H, Takasu S, Ban H, Kumagai T, Inada K, et al. Inhibitory effect of nordihydroguaiaretic acid, a plant lignan, on *Helicobacter pylori*-associated gastric carcinogenesis in Mongolian gerbils. Cancer Sci 2007;98:1689–95.
27. Cao X, Tsukamoto T, Seki T, Tanaka H, Morimura S, Cao L, Mizoshita T, Ban H, Toyoda T, Maeda H, Tatematsu M. 4-Vinyl-2,6-dimethoxyphenol (canolol) suppresses oxidative stress and gastric carcinogenesis in *Helicobacter pylori*-infected carcinogen-treated Mongolian gerbils. Int J Cancer 2008;122:1445–54.
28. Shimizu N, Inada KI, Tsukamoto T, Nakanishi H, Ikehara Y, Yoshikawa A, Kaminishi M, Kuramoto S, Tatematsu M. New animal model of glandular stomach carcinogenesis in Mongolian gerbils infected with *Helicobacter pylori* and treated with a chemical carcinogen. J Gastroenterol 1999;34(Suppl 11):61–6.
29. Tsukamoto T, Fukami H, Yamanaka S, Yamaguchi A, Nakanishi H, Sakai H, Aoki I, Tatematsu M. Hexosaminidase-altered aberrant crypts, carrying decreased hexosaminidase alpha and beta subunit mRNAs, in colon of 1,2-dimethylhydrazine-treated rats. Jpn J Cancer Res 2001;92:109–18.
30. Dixon MF, Genta RM, Yardley JH, Correa P. Classification and grading of gastritis. The updated Sydney System. International Workshop on the Histopathology of Gastritis, Houston 1994. Am J Surg Pathol 1996;20:1161–81.
31. Ikeno T, Ota H, Sugiyama A, Ishida K, Katsuyama T, Genta RM, Kawasaki S. *Helicobacter pylori*-induced chronic active gastritis, intestinal metaplasia, and gastric ulcer in Mongolian gerbils. Am J Pathol 1999;154:951–60.
32. Tanaka T, Kohno H, Suzuki R, Hata K, Sugie S, Niho N, Sakano K, Takahashi M, Wakabayashi K. Dextran sodium sulfate strongly promotes colorectal carcinogenesis in Apc(Min/+) mice: inflammatory stimuli by dextran sodium sulfate results in development of multiple colonic neoplasms. Int J Cancer 2006;118:25–34.
33. Kudo T, Lu H, Wu JY, Ohno T, Wu MJ, Genta RM, Graham DY, Yamaoka Y. Pattern of transcription factor activation in *Helicobacter pylori*-infected Mongolian gerbils. Gastroenterology 2007;132:1024–38.
34. Kim M, Miyamoto S, Yasui Y, Oyama T, Murakami A, Tanaka T. Zerumbone, a tropical ginger sesquiterpene, inhibits colon and lung carcinogenesis in mice. Int J Cancer 2009;124:264–71.
35. Tsukamoto T, Inada K, Tanaka H, Mizoshita T, Mihara M, Ushijima T, Yamamura Y, Nakamura S, Tatematsu M. Down-regulation of a gastric transcription factor. Sox2, and ectopic expression of intestinal homeobox genes Cdx1 and Cdx2: inverse correlation during progression from gastric/intestinal-mixed to complete intestinal metaplasia. J Cancer Res Clin Oncol 2004;130:135–45.
36. Fitzpatrick LR, Wang J, Le T. Caffeic acid phenethyl ester, an inhibitor of nuclear factor-κB, attenuates bacterial peptidoglycan polysaccharide-induced colitis in rats. J Pharmacol Exp Ther 2001;299:915–20.
37. Naumann M, Crabtree JE. *Helicobacter pylori*-induced epithelial cell signalling in gastric carcinogenesis. Trends Microbiol 2004;12:29–36.
38. Cao X, Tsukamoto T, Nozaki K, Tanaka H, Cao L, Toyoda T, Takasu S, Ban H, Kumagai T, Tatematsu M. Severity of gastritis determines glandular stomach carcinogenesis in *Helicobacter pylori*-infected Mongolian gerbils. Cancer Sci 2007;98:478–83.
39. Naito Y, Yoshikawa T. Molecular and cellular mechanisms involved in *Helicobacter pylori*-induced inflammation and oxidative stress. Free Radic Biol Med 2002;33:323–36.

40. D'Elios MM, Manghetti M, De Carli M, Costa F, Baldari CT, Burroni D, Telford JL, Romagnani S, Del Prete G. T helper 1 effector cells specific for *Helicobacter pylori* in the gastric antrum of patients with peptic ulcer disease. J Immunol 1997;158:962–7.
41. Karin M, Greten FR. NF-κB: linking inflammation and immunity to cancer development and progression. Nat Rev Immunol 2005;5:749–59.
42. Rajnakova A, Moochhala S, Goh PM, Ngoi S. Expression of nitric oxide synthase, cyclooxygenase, and p53 in different stages of human gastric cancer. Cancer Lett 2001;172:177–85.
43. Jackson LM, Wu KC, Mahida YR, Jenkins D, Hawkey CJ. Cyclooxygenase (COX) 1 and 2 in normal, inflamed, and ulcerated human gastric mucosa. Gut 2000;47:762–70.
44. Toyoda T, Tsukamoto T, Hirano N, Mizoshita T, Kato S, Takasu S, Ban H, Tatematsu M. Synergistic upregulation of inducible nitric oxide synthase and cyclooxygenase-2 in gastric mucosa of Mongolian gerbils by a high-salt diet and *Helicobacter pylori* infection. Histol Histopathol 2008;23:593–9.
45. Mizuno H, Sakamoto C, Matsuda K, Wada K, Uchida T, Noguchi H, Akamatsu T, Kasuga M. Induction of cyclooxygenase 2 in gastric mucosal lesions and its inhibition by the specific antagonist delays healing in mice. Gastroenterology 1997;112: 387–97.
46. Crabtree JE. Role of cytokines in pathogenesis of *Helicobacter pylori*-induced mucosal damage. Dig Dis Sci 1998;43:46S–55S.
47. Bodger K, Wyatt JI, Heatley RV. Gastric mucosal secretion of interleukin-10: relations to histopathology. *Helicobacter pylori* status, and tumour necrosis factor-alpha secretion. Gut 1997;40:739–44.
48. Nagashima R, Maeda K, Yuda F, Kudo K, Saitoh M, Takahashi T. *Helicobacter pylori* antigen in the glomeruli of patients with membranous nephropathy. Virchows. Arch 1997;431:235–9.
49. Sugimoto M, Sakai K, Kita M, Imanishi J, Yamaoka Y. Prevalence of *Helicobacter pylori* infection in long-term hemodialysis patients. Kidney Int 2009;75:96–103.

Pitavastatin Fails to Lower Serum Lipid Levels or Inhibit Gastric Carcinogenesis in *Helicobacter pylori*–Infected Rodent Models

Takeshi Toyoda,[1] Tetsuya Tsukamoto,[1] Shinji Takasu,[1] Naoki Hirano,[1] Hisayo Ban,[1] Liang Shi,[1] Toshiko Kumagai,[3] Takuji Tanaka[4] and Masae Tatematsu[1,2]

Abstract Statins are commonly used lipid-lowering drugs that reduce the risk of cardiovascular morbidity and mortality. Although recent studies have pointed to chemopreventive effects of statins against various cancers, their efficacy for gastric cancer is unclear. Here, we examined the effects of pitavastatin, a lipophilic statin, on *Helicobacter pylori* (*H. pylori*)–associated stomach carcinogenesis and gastritis using Mongolian gerbil and mouse models. The animals were allocated to *H. pylori* + *N*-methyl-*N*-nitrosourea administration (gerbils, 52 weeks) or *H. pylori* infection alone groups (gerbils and mice, 12 weeks). After *H. pylori* infection, they were fed basal diets containing 0 to 10 ppm of pitavastatin. The incidences of *H. pylori*–associated gastric adenocarcinomas and degrees of chronic gastritis were not decreased by pitavastatin compared with those of control values. Expression of interleukin-1β and tumor necrosis factor-α mRNAs in the pyloric mucosa was markedly up-regulated in pitavastatin-treated animals. Furthermore, in the *H. pylori*–infected groups, serum total cholesterol, triglyceride, and low-density lipoprotein levels were significantly increased by pitavastatin treatment, contrary to expectation. In the short-term study, *H. pylori*–infected gerbils and mice also showed significant up-regulation of serum triglyceride levels by pitavastatin, whereas total cholesterol was markedly reduced and low-density lipoprotein exhibited a tendency for decrease in noninfected animals. These findings indicate pitavastatin to be ineffective for suppressing gastritis and chemoprevention of gastric carcinogenesis in *H. pylori*–infected gerbils. Our serologic results also suggest that the *H. pylori* infection and consequent severe chronic gastritis interfere with the cholesterol-lowering effects of pitavastatin.

Statins are widely used drugs for the treatment of hypercholesterolemia, with beneficial effects on cardiovascular disease (1, 2). They are potent inhibitors of 3-hydroxy-3-methylglutaryl CoA reductase, a rate-limiting enzyme in cholesterol biosynthesis, and decrease serum lipid levels, especially low-density lipoprotein (LDL) cholesterol and triglyceride (TG). Recent studies have shown multifunctionality of statins, including anti-inflammatory and antiangiogenic effects, independent of their lipid-lowering influence (3, 4). Epidemiologic research has also suggested chemopreventive properties for various types of cancer, including colorectal tumors (5–7). However, studies of cancer prevention by statins have produced conflicting results (8–12).

Stomach cancer is the fourth most common cancer and second leading cause of cancer-related death worldwide (13). In spite of its importance, no large epidemiologic research into inhibitory effects of statin on stomach carcinogenesis has thus far been conducted. Moreover, there has been no *in vivo* examination of gastric carcinogenesis using animal models, although several rodent studies have shown statins to be preventive agents for colorectal cancer (14, 15). *Helicobacter pylori* (*H. pylori*) is now recognized as a major risk factor for chronic active gastritis and stomach cancer development (16, 17). In addition, it has been suggested to be also associated with coronary heart disease due to the alteration of the serum lipid profile (18, 19). Therefore, there is a possibility that *H. pylori* infection might influence the pharmacologic activity of statins.

The Mongolian gerbil (*Meriones unguiculatus*) provides a useful animal model of *H. pylori*–induced chronic active gastritis, allowing investigation of morbidity-related pathologic epithelial alterations in gastric mucosa and their development into gastric neoplasia (20). The purpose of the present study

Authors' Affiliations: [1]Division of Oncological Pathology, Aichi Cancer Center Research Institute; [2]Division of Cancer Genetics, Nagoya University Graduate School of Medicine, Nagoya, Japan; [3]Central Clinical Laboratories, Shinshu University Hospital, Matsumoto, Japan; and [4]1st Department of Pathology, Kanazawa Medical University, Ishikawa, Japan

Received 2/17/09; revised 4/20/09; accepted 5/11/09; published OnlineFirst 7/21/09.

Grant support: Grant-in-Aid for the Third-term Comprehensive 10-year Strategy for Cancer Control; Grant-in-Aid for Cancer Research from the Ministry of Health, Labour and Welfare, Japan; and Grant-in-Aid from the Ministry of Education, Culture, Sports, Science and Technology, Japan.

Requests for reprints: Tetsuya Tsukamoto, Division of Oncological Pathology, Aichi Cancer Center Research Institute, 1-1 Kanokoden, Chikusa-ku, Nagoya 464-8681, Japan. Phone: 81-52-762-6111; Fax: 81-52-764-2972; E-mail: ttsukamt@aichi-cc.jp.

doi:10.1158/1940-6207.CAPR-09-0082

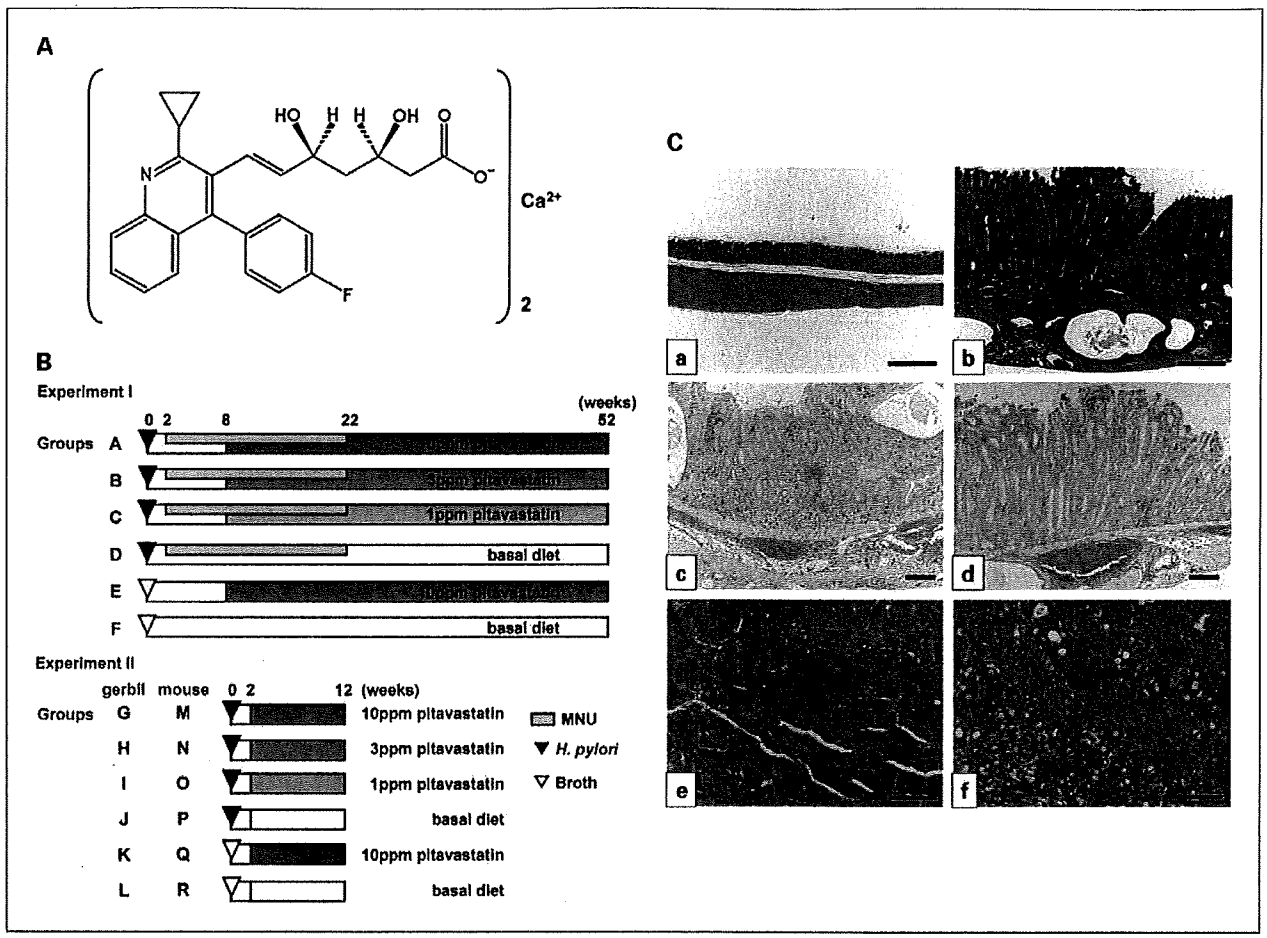

Fig. 1. *A*, chemical structure of pitavastatin. $C_{50}H_{46}CaF_2N_2O_8$ (molecular weight, 880.98). *B*, experimental design. Six-week-old male Mongolian gerbils or C57BL/6J mice were inoculated with *H. pylori* (ATCC43504 strain for gerbils or SS1 strain for mice) or Brucella broth. In the long-term experiment (experiment I), the gerbils (groups A-F) were given 10 ppm MNU in their drinking water for 20 wk and basal diet (CE-2) containing pitavastatin (0, 1, 3, or 10 ppm) from weeks 8 to 52. In the short-term experiment (experiment II), the gerbils (groups G-L) and mice (groups M-R) were given CE-2 diet containing pitavastatin from weeks 2 to 12. *C*, histopathology and immunohistochemistry in experiment I. a, normal gastric mucosa in a group F (untreated control group) gerbil at 52 wk (H&E). Magnification, ×30. *Bar*, 500 μm. b, marked infiltration of inflammatory cells and hyperplasia is evident in a group D (*H. pylori* + MNU) gerbil at 52 wk after infection (H&E). Magnification, ×30. *Bar*, 500 μm. c and d, note that the intensity of iNOS immunoreactivity in a group A (*H. pylori* + MNU + 10 ppm pitavastatin) gerbil is higher than that in a group D gerbil. Magnification, ×50 (*c* and *d*). *Bar*, 200 μm. e, well-differentiated adenocarcinoma in the glandular stomach of a group D gerbil (H&E). Magnification, ×160. *Bar*, 100 μm. f, poorly differentiated adenocarcinoma at 52 wk in a group D gerbil (H&E). Magnification, ×200. *Bar*, 100 μm.

was to evaluate the effect of pitavastatin, a recently developed lipophilic statin (21), on *H. pylori*–associated gastric carcinogenesis, and to clarify the effect of *H. pylori* infection and associated chronic gastritis on cholesterol-lowering effects of pitavastatin, using two rodent models.

Materials and Methods

Chemicals and diets

Pitavastatin (Fig. 1A) was kindly donated by Kowa Pharmaceutical Co. Ltd. CE-2 powder diet was purchased from Clea Japan, Inc. Experimental diets containing pitavastatin were prepared every 8 d in our laboratory and stored in a refrigerator. Food cups were replenished with fresh diet every second day. The gastric carcinogen *N*-methyl-*N*-nitrosourea (MNU) was purchased from Sigma Chemical, dissolved in distilled water at the concentration of 10 ppm, and administered via light-shielded bottles in drinking water *ad libitum*. MNU solutions were freshly prepared thrice per week.

Inoculation of *H. pylori*

H. pylori was prepared by the same method as described previously (22). Briefly, *H. pylori* strain ATCC43504 or Sydney strain 1 (American Type Culture Collection) was grown in Brucella broth (Becton Dickinson), containing 7% (v/v) heat-inactivated fetal bovine serum, at 37°C under microaerophilic conditions using an Anaero Pack Campylo (Mitsubishi Gas Chemical Co., Inc.) at high humidity for 24 h. After 24-h fasting, animals were inoculated via an oral catheter with 1.0 mL (gerbils) or 0.8 mL (mice) of aliquots of *H. pylori* culture containing 1.0×10^8 colony-forming units/mL of the organisms. Before inoculation, the broth cultures of *H. pylori* were checked under a phase-contrast microscope (TMS; Nikon Co.) for bacterial shape and mobility. Four hours later, the animals were again allowed free access to food.

Animals and experimental protocol

Two hundred thirty-three specific pathogen-free male Mongolian gerbils (MGS/Sea; Kyudo Co. Ltd.) and 118 specific pathogen-free male C57BL/6J mice (Clea Japan), 6 wk old, were used in this study.

All animals were housed in plastic cages on hardwood chip bedding in an air-conditioned biohazard room with a 12-h light/12-h dark cycle and allowed free access to food and water. The experimental designs were approved by the Animal Care Committee of the Aichi Cancer Center Research Institute, and the animals were cared for in accordance with institutional guidelines as well as the Guidelines for Proper Conduct of Animal Experiments (Science Council of Japan, June 1, 2006). The experimental design is illustrated in Fig. 1B. The animals were allocated to experiments I and II.

In experiment I, 175 gerbils were divided into six groups (groups A-F). Two weeks after inoculation of *H. pylori*, gerbils of groups A to D were administered MNU for 20 wk, and groups E and F were given broth and autoclaved distilled water. From weeks 8 to 52, the gerbils received CE-2 diets containing pitavastatin at concentrations of 10 (groups A and E), 3 (group B), 1 (group C), or 0 ppm (groups D and F). All surviving animals were sacrificed under deep anesthesia at 52 wk after inoculation and subjected to laparotomy with excision of the stomach.

In experiment II, a total of 58 gerbils and 118 mice were divided into six groups (groups G-L and M-R, respectively). Groups G to J and M to P were inoculated with *H. pylori* as in experiment I. From weeks 2 to 12, the animals received CE-2 diet containing pitavastatin at the concentrations of 10 (groups G, K, M, and Q), 3 (groups H and N), 1 (groups I and O), or 0 ppm (groups J, L, P, and R). Sacrifice was at 12 wk after inoculation.

Histology and immunohistochemistry

For histologic and immunohistochemical examination, the stomachs were fixed in 10% neutral-buffered formalin for 24 h, sliced along the longitudinal axis into strips of equal width, and embedded in paraffin. Serial sections (4 μm thick) were prepared and stained with H&E for morphologic observation and immunohistochemistry for cyclooxygenase-2 (COX-2) and inducible nitric oxide synthase (iNOS). The degree of chronic active gastritis was graded according to criteria modified from the updated Sydney System (23), by scoring the infiltration of neutrophils and mononuclear cells, as well as intestinal metaplasia and heterotopic proliferative glands (HPGs), on a four-point scale (0-3; 0, normal; 1, mild; 2, moderate; 3, marked). Immunohistochemical analysis of COX-2 and iNOS was carried out with a mouse monoclonal anti–COX-2 antibody (diluted 1:200; BD Biosciences) and a rabbit polyclonal anti-iNOS antibody (1:500; Calbiochem) as previously described (24). To quantitate the degree of staining, the grading system used the following criteria: grade 0 (negative), grades 1 to 3 (increasing degrees of intermediate immunoreactivity), and grade 4 (extensive reactivity; ref. 25). The sections were analyzed on BX50 light microscope (Olympus). Images were captured using AxioVision 4.6 software (Carl Zeiss Co. Ltd.) and further processed with Adobe Photoshop software (Adobe Systems).

Serologic examination

Before removal of the stomachs, blood samples were collected from the inferior vena cava after laparotomy. Sera were separated from blood and the total cholesterol (T-Chol), TG, high-density lipoprotein (HDL), and LDL levels were measured by ELISA (SRL, Inc.). The titers of anti–*H. pylori* antibodies were also determined with an ELISA kit (Biomerica) and values were expressed using an arbitrary index (26).

Analysis of mRNA expression of inflammatory factors by real-time quantitative PCR

Total RNA was extracted from the antrum and corpus in the glandular stomach of gerbils using a QuickGene RNA Tissue Kit SII (Fujifilm). After DNase treatment, first-strand cDNAs were synthesized using a SuperScript III First-Strand Synthesis System for reverse transcription-PCR (Invitrogen) according to the manufacturer's instructions. Quantitative PCR of interleukin (IL)-1β, tumor necrosis factor (TNF)-α, and iNOS was done using a StepOne Real-Time PCR System (Applied Biosystems) with the gerbil-specific *glyceraldehyde-3-phosphate dehydrogenase* gene as an internal control. The PCR was done basically following the manufacturer's instructions using a QuantiTect SYBR Green PCR kit (Qiagen). For PCR amplification, the following primers were used: glyceraldehyde-3-phosphate dehydrogenase, 5′-AACGGCACAGTCAAGGCTGAGAACG-3′ and 5′-CAACATACTCGGCACCGGCATCG-3′; IL-1β, 5′-TTGGGCCTCAAGGGAAAGAATCTGT-3′ and 5′-GGTATTGTTTGGGGTCCACGCTCTC-3′; TNF-α, 5′-GCCCCCACCTCGTGCTCCTCAC-3′ and 5′-GGCAGGGGCTCTTGATGGCAGACAG-3′; and iNOS, 5′-GCTTGAGCGAGGAGCAGGTTGAGGA-3′ and 5′-CGCTGGCCTTTTTCACCCCATAGGA-3′. Specificity of the PCR was confirmed using a melt curve program provided with the StepOne software. To further confirm that there was no obvious primer dimer formation or amplification of any extra bands, the samples were electrophoresed in 3% agarose gels and visualized with ethidium bromide after the StepOne reaction. Relative quantification was done as previously established using the internal control without the necessity for external standards (27). The expression levels of mRNAs were expressed relative to 1.0 in the control group.

Table 1. Summary of the general data and incidences of gastric carcinomas in Mongolian gerbils in experiment I

Group (*n*)	Treatment	BW (g)	Anti-Hp IgG titer (AI)	Relative organ weights (%)		Adenocarcinoma		
				Liver	Kidney	Well	Por	Incidence (%)
A (40)	Hp + MNU + 10 ppm PS	96.6 ± 14.9	257.8 ± 225.4	5.09 ± 0.81*	0.85 ± 0.06	15	3	18/40 (45.0)
B (39)	Hp + MNU + 3 ppm PS	97.3 ± 9.4	415.4 ± 452.3	5.08 ± 0.77*	0.84 ± 0.07	22	0	22/39 (56.4)
C (40)	Hp + MNU + 1 ppm PS	89.1 ± 16.6	233.6 ± 218.3	4.76 ± 1.00*	0.85 ± 0.07	19	1	20/40 (50.0)
D (41)	Hp + MNU	91.5 ± 14.9	296.5 ± 197.7	4.73 ± 1.03*	0.85 ± 0.11	15	2	17/41 (41.5)
E (10)	Broth + 10 ppm PS	94.7 ± 9.7	3.8 ± 3.2	3.84 ± 0.11	0.71 ± 0.06*	0	0	0/10 (0)
F (5)	Untreated control	89.7 ± 12.9	ND	3.65 ± 0.31	0.83 ± 0.07	0	0	0/5 (0)

NOTE: Values for results are expressed as mean ± SD.

Abbreviations: BW, body weight; Hp, *Helicobacter pylori*; AI, arbitrary index; Well, well-differentiated adenocarcinoma; Por, poorly differentiated adenocarcinoma; PS, pitavastatin; ND, not done.

*$P < 0.01$ versus group F.

Table 2. Body weights and histopathologic evaluation of gastritis in Mongolian gerbils and mice in experiment II

Animal	Group (*n*)	Treatment	BW (g)	Scores of gastritis			
				Infiltration of neutrophils		Infiltration of mononuclear cells	
				Antrum	Corpus	Antrum	Corpus
Gerbils	G (10)	Hp + 10 ppm PS	76.4 ± 4.5	2.3 ± 0.5	1.6 ± 0.9	2.4 ± 0.4	1.9 ± 0.5
	H (10)	Hp + 3 ppm PS	74.2 ± 10.6	2.2 ± 0.4	1.9 ± 1.1	2.5 ± 0.5	2.0 ± 0.8
	I (10)	Hp + 1 ppm PS	74.3 ± 7.7	2.4 ± 0.4	1.6 ± 0.8	2.5 ± 0.4	2.0 ± 0.8
	J (10)	Hp	70.8 ± 8.2	2.3 ± 0.4	1.2 ± 0.9	2.7 ± 0.2	1.7 ± 0.7
	K (8)	Broth + 10 ppm PS	73.8 ± 4.2	0.0 ± 0.0	0.0 ± 0.0	0.1 ± 0.2	0.1 ± 0.2
	L (10)	Broth	75.2 ± 6.4	0.1 ± 0.2	0.0 ± 0.0	0.2 ± 0.2	0.0 ± 0.0
Mice	M (19)	Hp + 10 ppm PS	30.2 ± 2.2	1.0 ± 0.3	1.3 ± 0.6	0.9 ± 0.2	1.2 ± 0.4
	N (19)	Hp + 3 ppm PS	30.5 ± 2.0	1.1 ± 0.3	1.4 ± 0.4	1.0 ± 0.2	1.3 ± 0.4
	O (19)	Hp + 1 ppm PS	30.4 ± 1.8	0.8 ± 0.3	1.0 ± 0.5	0.8 ± 0.3	1.1 ± 0.5
	P (20)	Hp	28.9 ± 2.8	1.0 ± 0.5	1.2 ± 0.6	0.8 ± 0.3	1.0 ± 0.5
	Q (21)	Broth + 10 ppm PS	29.2 ± 1.8	0.0 ± 0.1	0.2 ± 0.3	0.0 ± 0.0	0.0 ± 0.1
	R (20)	Broth	28.4 ± 1.0	0.1 ± 0.2	0.4 ± 0.5	0.0 ± 0.0	0.0 ± 0.0

NOTE: Values for results are expressed as mean ± SD.

Statistical analysis

The Fisher's exact test was used to assess incidences of gastric adenocarcinomas. Quantitative values were expressed as mean ± SD or SE, and differences between means were statistically analyzed by the ANOVA or Kruskal-Wallis followed by the multiple comparison test. P values of <0.05 were considered to be statistically significant.

Results

Average body weights, titer of anti-*H. pylori* antibodies, and relative organ weights

Data for average body weights, titer of anti-*H. pylori* antibodies, and relative organ weights in the long-term experiment (experiment I) and average body weights in the short-term experiment (experiment II) are shown in Tables 1 and 2, respectively. There was no significant variation of body weights in experiments I and II. In experiment I, all *H. pylori*–infected groups (groups A-D) showed significantly higher values for anti-*H. pylori* antibody titers than the noninfected group (group E). The relative liver weights in groups A to D were markedly higher than in nontreated control group (group F). The relative kidney weights in group E were statistically decreased compared with group F. In internal organs other than the stomach, including the liver, kidney, spleen, heart, and lung of all groups (groups A-F), no macroscopic or microscopic lesions were observed.

Status of gastritis

All gastric mucosal specimens from uninfected gerbils and mice had normal histomorphology (Fig. 1C, *a*). Histologic findings for chronic gastritis in experiments I (Table 3) and II (Table 2) are summarized. The long-term *H. pylori*–infected gerbils showed severe gastritis with intestinal metaplasia and HPGs (Fig. 1C, *b*). There were no significant differences in inflammatory scores, including infiltration of neutrophils or mononuclear cells, intestinal metaplasia, and HPGs, both in the antrum and corpus, among all infected groups in experiment I. In experiment II, the infiltration of neutrophils and mononuclear cells of short-term *H. pylori*–infected gerbils was greater than that in mice. There were no statistically significant differences in the degree of inflammation among *H. pylori*–infected animals, as in experiment I. In experiment I, the score for iNOS immunohistochemistry in group A (*H. pylori* + MNU + 10 ppm pitavastatin) was markedly higher than that in group D (*H. pylori* + MNU) both in the antrum and corpus (Fig. 1C, *c* and *d*).

Incidences of glandular stomach adenocarcinomas

In experiment I, both well-differentiated and poorly differentiated adenocarcinomas were found in *H. pylori*–infected and MNU-treated groups (groups A-D) at 52 weeks after infection (Fig. 1C, *e* and *f*). However, there were no significant differences in the incidences among groups A to D [group A, 45.0% (18 of 40); group B, 56.4% (22 of 39); group C, 50.0% (20 of 40); group D, 41.5% (17 of 41); Table 1]. In noninfected control groups (groups E and F) and short-term infected groups (experiment II), no tumors developed in the stomach.

Serologic results

On serologic examination, pitavastatin treatment significantly increased serum T-Chol, TG, and LDL levels in *H. pylori*–infected gerbils in a dose-dependent manner (groups A-D) in the long-term experiment (experiment I; Fig. 2). Similarly, in noninfected animals (groups E and F), serum LDL levels were increased by 10 ppm pitavastatin treatment. On the other hand, HDL levels were markedly reduced in both group D (*H. pylori* + MNU) and group E (10 ppm pitavastatin) compared with group F (untreated control).

In experiment II, serum TG and HDL levels showed significant up-regulation by pitavastatin treatment in *H. pylori*–infected gerbils (groups G-J). In contrast, T-Chol and HDL

levels were markedly decreased by 10 ppm pitavastatin in noninfected gerbils (groups K and L). In *H. pylori*–infected mice (groups M-P), serum TG levels were significantly increased by pitavastatin, as in the gerbil case. In noninfected mice (groups Q and R), the serum LDL level showed a tendency for decrease with 10 ppm pitavastatin treatment, although this was not statistically significant ($P = 0.063$).

Administration of pitavastatin and mRNA expression of IL-1β, TNF-α, and iNOS

Gastric IL-1β, TNF-α, and iNOS mRNA were found to be expressed at very low levels in the noninfected control gerbils. However, in the *H. pylori*–infected animals, the levels of these inflammatory factors were markedly elevated in the antrum and corpus (Fig. 3A and B). In the long-term experiment (experiment I), relative expression of IL-1β and TNF-α in the antrum of pitavastatin-treated groups (groups A-C) was significantly up-regulated compared with the untreated group (group D; Fig. 3A).

Discussion

The present study did not provide any evidence of statin protection against gastritis or gastric carcinogenesis in two animal models. The relationship between statin use and cancer incidence has been evaluated in numerous epidemiologic studies. Some reports supported a role in cancer chemoprevention (6, 28), and others refuted the hypothesis (29). Recently, Lubet et al. (30) suggested that atorvastatin and lovastatin fail to inhibit mammary carcinogenesis of rodents. In case of gastrointestinal cancer, clinical studies of statins for preventive effects have also produced conflicting results (31). Statins are the most widely used drugs both in the amounts prescribed and the proceeds of sales (32), so we need to clarify whether they are truly effective for cancer chemoprevention. Here, we showed that *H. pylori*–associated gastric carcinogenesis in Mongolian gerbils is not prevented by oral administration of pitavastatin at 10 ppm in the diet. We selected the pitavastatin as a strong candidate to alleviate gastritis and gastric carcinogenesis as well as to lower the serum lipid levels because pitavastatin has more potent lipid-lowering effects than pravastatin, simvastatin, and atorvastatin (21, 33). Furthermore, pitavastatin has been known to be minimally affected by cytochrome *P*450 3A4 inhibitors unlike simvastatin, lovastatin, and atorvastatin (34). Because cytochrome *P*450 metabolisms in gerbils have not been fully clarified yet, we selected pitavastatin to avoid species difference in the drug metabolism in this experiment. Among mice strains, C57BL/6 mice showed excellent colonization of *H. pylori* in the antrum, whereas BALB/c and CBA mice showed only mild gastritis (35); thus, the former was chosen here. Pitavastatin has been shown to prevent digestive system carcinogenesis, such as colorectal and lingual cancer, in mouse models (14, 36); however, the degree of gastritis in our study was not attenuated by pitavastatin in *H. pylori*–infected gerbils and mice. The major determining factor of stomach carcinogenesis is the severity of *H. pylori*–induced gastritis (37). Therefore, the ineffectiveness of pitavastatin regarding prevention of gastric cancer development in the gerbil model might be due to the lack of suppressive effects on *H. pylori*–induced gastritis.

In the long-term experiment, interestingly, our data suggested that the serum lipid levels (T-Chol, TG, and LDL) of *H. pylori*–infected and MNU-treated gerbils were significantly increased by pitavastatin in a dose-dependent manner. In noninfected gerbils, similarly, values for LDL cholesterol level were markedly elevated by the statin, although the HDL cholesterol level was significantly decreased. It was expected that pitavastatin would lower the LDL without changing HDL levels. Therefore, we did the additional short-term experiment (experiment II) to clarify whether the effect of pitavastatin on serum lipid profile was influenced by *H. pylori* infection, MNU treatment, or biological trait of gerbils. Again, inflammatory

Table 3. Histopathologic evaluation of gastritis in Mongolian gerbils in experiment I

Group (*n*)	Treatment	Infiltration of neutrophils		Infiltration of mononuclear cells		Intestinal metaplasia		HPGs		COX-2 immunostaining		iNOS immunostaining	
		Antrum	Corpus	Antrum	Corpus	Antrum	Corpus	Antrum	Corpus	Antrum	Corpus	Antrum	Corpus
A (40)	Hp + MNU + 10 ppm PS	2.0±0.7	2.3±0.8	2.8±0.4	2.6±0.5	1.2±0.8	1.6±0.8	2.3±0.7	2.2±0.9	1.3±0.7	1.6±0.7	2.0±0.6*	1.8±0.6*
B (39)	Hp + MNU + 3 ppm PS	2.1±0.6	2.4±0.8	2.7±0.4	2.5±0.5	1.3±0.8	1.5±0.6	2.3±0.7	2.3±0.7	1.5±0.8	1.7±0.7	1.7±0.5	1.7±0.6
C (40)	Hp + MNU + 1 ppm PS	2.0±0.7	2.3±0.7	2.7±0.4	2.5±0.6	1.3±0.9	1.6±0.8	2.3±0.6	2.0±0.9	1.5±0.7	1.6±0.7	1.6±0.6	1.4±0.5
D (41)	Hp + MNU	1.8±0.6	2.1±0.8	2.6±0.5	2.4±0.5	1.0±0.7	1.2±0.7	2.1±0.7	1.9±0.8	1.6±0.8	1.5±0.6	1.5±0.6	1.4±0.5
E (10)	Broth + 10 ppm PS	0.0±0.0	0.0±0.0	0.3±0.4	0.0±0.0	0.0±0.0	0.0±0.0	0.0±0.0	0.0±0.0	0.0±0.0	0.0±0.0	0.1±0.3	0.0±0.0
F (5)	Untreated control	0.0±0.0	0.0±0.0	0.0±0.0	0.0±0.0	0.0±0.0	0.0±0.0	0.0±0.0	0.0±0.0	0.0±0.0	0.0±0.0	0.0±0.0	0.0±0.0

NOTE: Values for results are expressed as mean ± SD.
*$P < 0.01$ versus group D.

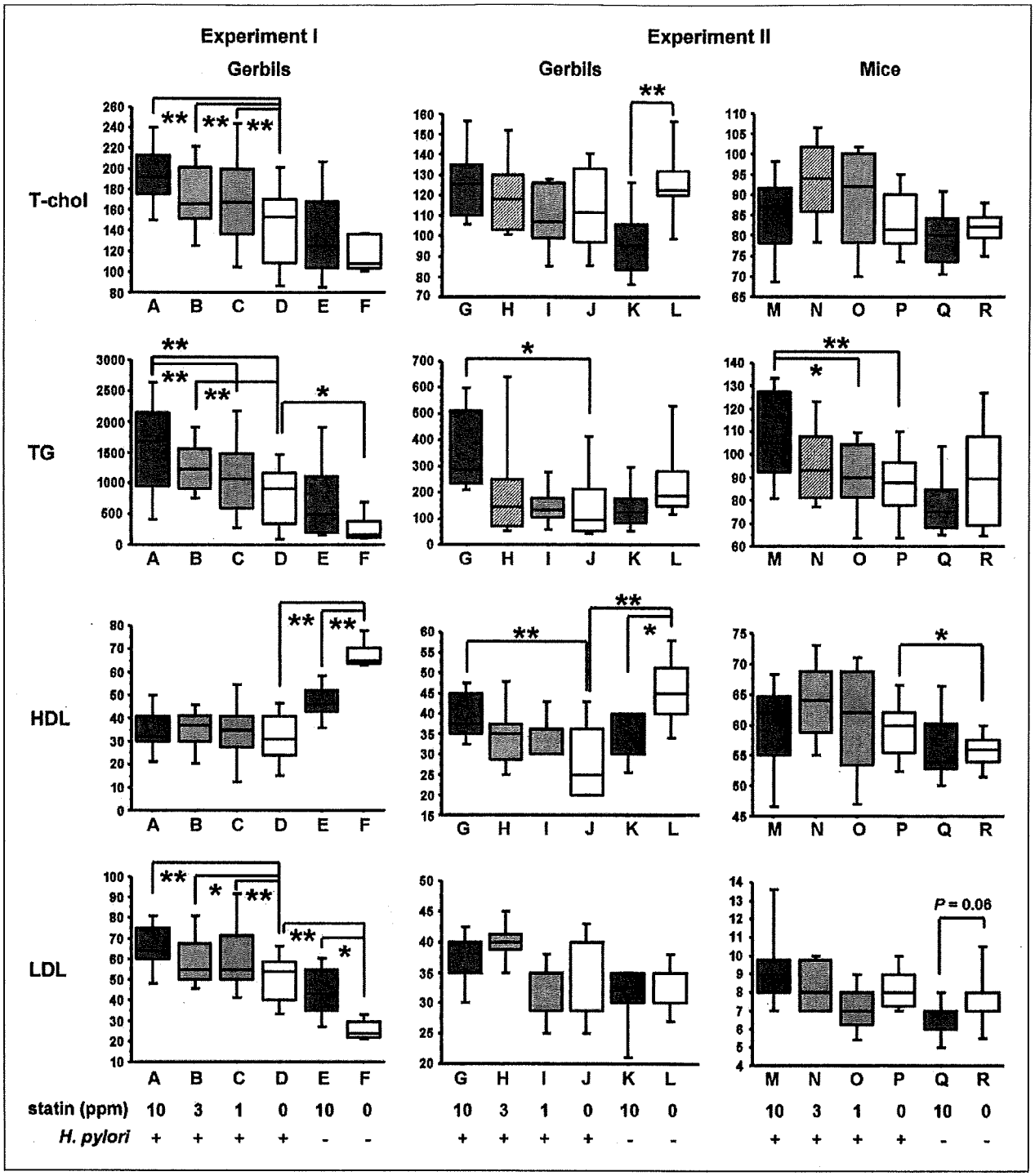

Fig. 2. Serologic results were depicted by box plots. *Line inside each box*, median; *boxes*, 25th and 75th percentiles; *error bars*, 90th and 10th percentiles. *, $P < 0.05$; **, $P < 0.01$.

scores for gastritis in *H. pylori*–infected gerbils and mice were not attenuated by pitavastatin, and serum TG levels were significantly increased. On the other hand, in the noninfected mice, LDL cholesterol showed tendency for decrease. Similarly, in noninfected gerbils, pitavastatin significantly reduced the serum T-Chol and HDL levels. These serologic results suggest that *H. pylori* infection might influence the effects of the statin. Oral administrated pitavastatin is absorbed mainly in the

duodenum and colon with a minimum metabolic change but partly in the stomach. Thus, there is a possibility that the pharmacokinetics of pitavastatin might be modified by *H. pylori*–induced severe chronic gastritis.

Some infectious diseases, such as *Chlamydia pneumoniae* infection, have been considered as risk factors for coronary heart disease (18), and several studies have pointed to an association between *H. pylori* infection and vascular changes due to the alteration of the serum lipid profile (19, 38). Previous studies reported that the serum T-Chol, TG, or LDL concentrations in *H. pylori*–infected persons are significantly elevated over those in noninfected individuals (39, 40). On the other hand, several authors described HDL cholesterol levels to be decreased by long-term infection with *H. pylori* (41–43). In the present study, *H. pylori*–infected animals showed similar lipid dynamics with significant elevation of TG and LDL and depression of HDL, and pitavastatin markedly up-regulated the T-Chol and TG levels in infected groups. Thus, our data support the hypothesis that the conversion of serum lipid dynamics caused by *H. pylori* infection influences the cholesterol-lowering effect of pitavastatin.

The antral mRNA expression levels of inflammatory cytokines (IL-1β and TNF-α) were found to be significantly increased by pitavastatin treatment in *H. pylori*–infected and MNU-treated gerbils, although there were no significant differences in inflammatory scores. In addition, the immunoreactivity scores of iNOS both in the antrum and corpus of these gerbils were higher than those of control (*H. pylori* + MNU) gerbils. Recently, Habara et al. (44) showed that pitavastatin up-regulates iNOS expression in cytokine-stimulated hepatocytes. The findings described here suggest potential enhancing effects of statins on *H. pylori*–induced gastritis through up-regulation of these inflammatory factors, in contrast to the anti-inflammatory effects reported in colon.

Statins are well recognized as relatively safe drugs, although adverse effects include hepatotoxicity and myopathy at low incidence. In the present study, there was no significant variation in body weights with pitavastatin treatment in either *H. pylori*–infected or noninfected animals. No macroscopic lesions in the liver, spleen, kidney, heart, lung, pancreas, testis, and skeletal muscles were observed. In addition, histologic examination revealed no pathologic findings in the liver, spleen, kidney, heart, lung, and skeletal muscles

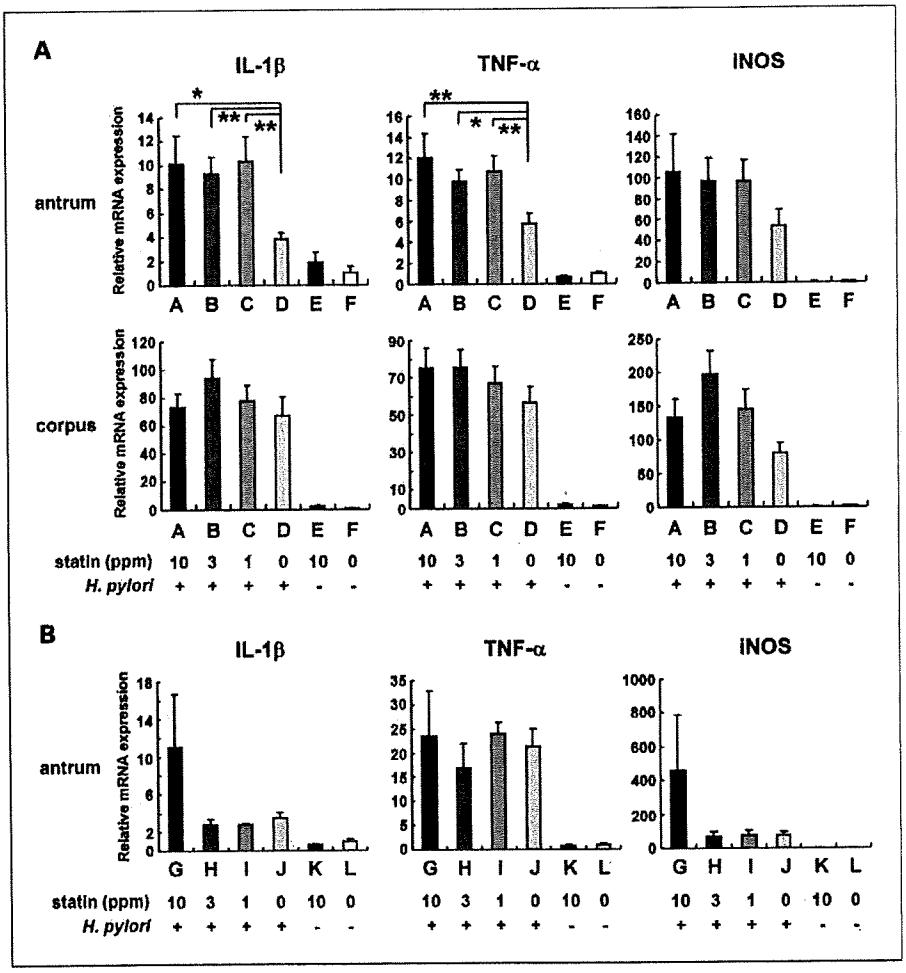

Fig. 3. Relative expression levels of IL-1β, TNF-α, and iNOS mRNAs in the gastric mucosa. *A*, expression in the antrum and corpus of gerbils at 52 wk after infection. Columns, mean arbitrary units relative to 1.0 for controls (group F); bars, SE. Note increase in groups A to C (pitavastatin-treated groups) compared with group D (*H. pylori*–infected control group), especially in the antrum. *, $P < 0.05$; **, $P < 0.01$. *B*, expression levels in the antrum of glandular stomachs of gerbils at 12 wk after infection. Columns, mean arbitrary units relative to 1.0 for controls (group L); bars, SE. Note increase in group G (10 ppm pitavastatin–treated gerbils) compared with group J (*H. pylori*–infected control gerbils), although statistically significant differences are lacking among groups G to J.

of gerbils at 52 weeks. Therefore, it was considered that pitavastatin toxicity was lacking or limited at the dose used in the present study.

In conclusion, pitavastatin does not seem to be associated with reduced risk of stomach carcinogenesis in *H. pylori*–infected Mongolian gerbils. Furthermore, *H. pylori* infection interferes with the serum lipid-lowering effects of pitavastatin in gerbil and mouse models. Our results therefore suggest that care is needed in use of statins for *H. pylori*–infected individuals, especially those with severe chronic gastritis. Large-scale epidemiologic studies should be recommended to determine whether statins have effects on stomach cancer development.

Disclosure of Potential Conflicts of Interest

No potential conflicts of interest were disclosed.

References

1. Hebert PR, Gaziano JM, Chan KS, Hennekens CH. Cholesterol lowering with statin drugs, risk of stroke, and total mortality. An overview of randomized trials. JAMA 1997;278:313–21.
2. Baigent C, Keech A, Kearney PM, et al. Efficacy and safety of cholesterol-lowering treatment: prospective meta-analysis of data from 90,056 participants in 14 randomised trials of statins. Lancet 2005;366:1267–78.
3. Dulak J, Jozkowicz A. Anti-angiogenic and anti-inflammatory effects of statins: relevance to anti-cancer therapy. Curr Cancer Drug Targets 2005;5:579–94.
4. Ito MK, Talbert RL, Tsimikas S. Statin-associated pleiotropy: possible beneficial effects beyond cholesterol reduction. Pharmacotherapy 2006;26: 85–101S.
5. Poynter JN, Gruber SB, Higgins PD, et al. Statins and the risk of colorectal cancer. N Engl J Med 2005;352:2184–92.
6. Demierre MF, Higgins PD, Gruber SB, Hawk E, Lippman SM. Statins and cancer prevention. Nat Rev Cancer 2005;5:930–42.
7. Chan KK, Oza AM, Siu LL. The statins as anticancer agents. Clin Cancer Res 2003;9:10–9.
8. Coogan PF, Smith J, Rosenberg L. Statin use and risk of colorectal cancer. J Natl Cancer Inst 2007; 99:32–40.
9. Browning DR, Martin RM. Statins and risk of cancer: a systematic review and metaanalysis. Int J Cancer 2007;120:833–43.
10. Dale KM, Coleman CI, Henyan NN, Kluger J, White CM. Statins and cancer risk: a meta-analysis. JAMA 2006;295:74–80.
11. Jacobs EJ, Rodriguez C, Brady KA, Connell CJ, Thun MJ, Calle EE. Cholesterol-lowering drugs and colorectal cancer incidence in a large United States cohort. J Natl Cancer Inst 2006;98:69–72.
12. Vinogradova Y, Hippisley-Cox J, Coupland C, Logan RF. Risk of colorectal cancer in patients prescribed statins, nonsteroidal anti-inflammatory drugs, and cyclooxygenase-2 inhibitors: nested case-control study. Gastroenterology 2007;133: 393–402.
13. Parkin DM, Bray F, Ferlay J, Pisani P. Global cancer statistics, 2002. CA Cancer J Clin 2005;55:74–108.
14. Yasui Y, Suzuki R, Miyamoto S, et al. A lipophilic statin, pitavastatin, suppresses inflammation-associated mouse colon carcinogenesis. Int J Cancer 2007;121:2331–9.
15. Swamy MV, Patlolla JM, Steele VE, Kopelovich L, Reddy BS, Rao CV. Chemoprevention of familial adenomatous polyposis by low doses of atorvastatin and celecoxib given individually and in combination to APCMin mice. Cancer Res 2006;66: 7370–7.
16. Uemura N, Okamoto S, Yamamoto S, et al. *Helicobacter pylori* infection and the development of gastric cancer. N Engl J Med 2001;345:784–9.
17. IARC Working Group on the Evaluation of Carcinogenic Risks to Humans Infection with *Helicobacter pylori*. Schistosomes, liver flukes and *Helicobacter pylori*. In: IARC monographs on the evaluation of carcinogenic risks to humans, vol. 61. Lyon: World Health Organization/International Agency for Research on Cancer; 1994. p. 177–241.
18. Patel P, Mendall MA, Carrington D, et al. Association of *Helicobacter pylori* and *Chlamydia pneumoniae* infections with coronary heart disease and cardiovascular risk factors. BMJ 1995;311:711–4.
19. Niemela S, Karttunen T, Korhonen T, et al. Could *Helicobacter pylori* infection increase the risk of coronary heart disease by modifying serum lipid concentrations? Heart 1996;75:573–5.
20. Sugiyama A, Maruta F, Ikeno T, et al. *Helicobacter pylori* infection enhances *N*-methyl-*N*-nitrosourea-induced stomach carcinogenesis in the Mongolian gerbil. Cancer Res 1998;58:2067–9.
21. Mukhtar RY, Reid J, Reckless JP. Pitavastatin. Int J Clin Pract 2005;59:239–52.
22. Shimizu N, Inada KI, Tsukamoto T, et al. New animal model of glandular stomach carcinogenesis in Mongolian gerbils infected with *Helicobacter pylori* and treated with a chemical carcinogen. J Gastroenterol 1999;34:61–6.
23. Dixon MF, Genta RM, Yardley JH, Correa P. Classification and grading of gastritis. The updated Sydney System. International Workshop on the Histopathology of Gastritis, Houston 1994. Am J Surg Pathol 1996;20:1161–81.
24. Tanaka T, Kohno H, Suzuki R, et al. Dextran sodium sulfate strongly promotes colorectal carcinogenesis in Apc(Min/+) mice: inflammatory stimuli by dextran sodium sulfate results in development of multiple colonic neoplasms. Int J Cancer 2006; 118:25–34.
25. Zingarelli B, Szabo C, Salzman AL. Reduced oxidative and nitrosative damage in murine experimental colitis in the absence of inducible nitric oxide synthase. Gut 1999;45:199–209.
26. Cao X, Tsukamoto T, Seki T, et al. 4-Vinyl-2,6-dimethoxyphenol (canolol) suppresses oxidative stress and gastric carcinogenesis in *Helicobacter pylori*-infected carcinogen-treated Mongolian gerbils. Int J Cancer 2008;122:1445–54.
27. Tsukamoto T, Fukami H, Yamanaka S, et al. Hexosaminidase-altered aberrant crypts, carrying decreased hexosaminidase α and β subunit mRNAs, in colon of 1,2-dimethylhydrazine-treated rats. Jpn J Cancer Res 2001;92:109–18.
28. Karp I, Behlouli H, Lelorier J, Pilote L. Statins and cancer risk. Am J Med 2008;121:302–9.
29. Kuoppala J, Lamminpaa A, Pukkala E. Statins and cancer: a systematic review and meta-analysis. Eur J Cancer 2008;44:2122–32.
30. Lubet RA, Boring D, Steele VE, Ruppert JM, Juliana MM, Grubbs CJ. Lack of efficacy of the statins atorvastatin and lovastatin in rodent mammary carcinogenesis. Cancer Prev Res 2009;2:161–7.
31. Bhuket TP, Higgins PD. Drug insight: statins and gastrointestinal cancer. Nat Clin Pract Gastroenterol Hepatol 2006;3:552–62.
32. Moorman PG, Hamilton RJ. Statins and cancer risk: what do we know and where do we go from here? Epidemiology 2007;18:194–6.
33. Saito Y, Yamada N, Teramoto T, et al. A randomized, double-blind trial comparing the efficacy and safety of pitavastatin versus pravastatin in patients with primary hypercholesterolemia. Atherosclerosis 2002;162:373–9.
34. Neuvonen PJ, Niemi M, Backman JT. Drug interactions with lipid-lowering drugs: mechanisms and clinical relevance. Clin Pharmacol Ther 2006;80: 565–81.
35. Sakagami T, Dixon M, O'Rourke J, et al. Atrophic gastric changes in both *Helicobacter felis* and *Helicobacter pylori* infected mice are host dependent and separate from antral gastritis. Gut 1996;39: 639–48.
36. Miyamoto S, Yasui Y, Kim M, et al. A novel rasH2 mouse carcinogenesis model that is highly susceptible to 4-NQO-induced tongue and esophageal carcinogenesis is useful for preclinical chemoprevention studies. Carcinogenesis 2008;29:418–26.
37. Cao X, Tsukamoto T, Nozaki K, et al. Severity of gastritis determines glandular stomach carcinogenesis in *Helicobacter pylori*-infected Mongolian gerbils. Cancer Sci 2007;98:478–83.
38. Pasceri V, Cammarota G, Patti G, et al. Association of virulent *Helicobacter pylori* strains with ischemic heart disease. Circulation 1998;97:1675–9.
39. Laurila A, Bloigu A, Nayha S, Hassi J, Leinonen M, Saikku P. Association of *Helicobacter pylori* infection with elevated serum lipids. Atherosclerosis 1999;142:207–10.
40. Kucukazman M, Yavuz B, Sacikara M, et al. The relationship between updated Sydney System score and LDL cholesterol levels in patients infected with *Helicobacter pylori*. Dig Dis Sci 2009; 54:604–7.
41. Takashima T, Adachi K, Kawamura A, et al. Cardiovascular risk factors in subjects with *Helicobacter pylori* infection. Helicobacter 2002;7:86–90.
42. Scragg RK, Fraser A, Metcalf PA. *Helicobacter pylori* seropositivity and cardiovascular risk factors in a multicultural workforce. J Epidemiol Community Health 1996;50:578–9.
43. Hoffmeister A, Rothenbacher D, Bode G, et al. Current infection with *Helicobacter pylori*, but not seropositivity to *Chlamydia pneumoniae* or cytomegalovirus, is associated with an atherogenic, modified lipid profile. Arterioscler Thromb Vasc Biol 2001;21:427–32.
44. Habara K, Hamada Y, Yamada M, et al. Pitavastatin up-regulates the induction of iNOS through enhanced stabilization of its mRNA in pro-inflammatory cytokine-stimulated hepatocytes. Nitric Oxide 2008;18:19–27.

 Related Commentary, page 81

Glucokinase and IRS-2 are required for compensatory β cell hyperplasia in response to high-fat diet–induced insulin resistance

Yasuo Terauchi,[1,2,3] Iseki Takamoto,[1,2,4] Naoto Kubota,[1,2,4] Junji Matsui,[1] Ryo Suzuki,[1,2] Kajuro Komeda,[5] Akemi Hara,[5] Yukiyasu Toyoda,[6] Ichitomo Miwa,[6] Shinichi Aizawa,[7] Shuichi Tsutsumi,[8] Yoshiharu Tsubamoto,[1] Shinji Hashimoto,[1] Kazuhiro Eto,[1,2] Akinobu Nakamura,[3] Mitsuhiko Noda,[2,4,9] Kazuyuki Tobe,[1,2] Hiroyuki Aburatani,[8] Ryozo Nagai,[10] and Takashi Kadowaki[1,2,4]

[1]Department of Metabolic Diseases, Graduate School of Medicine, University of Tokyo, Tokyo, Japan. [2]Core Research for Evolutional Science and Technology (CREST), Japan Science and Technology Corporation (JST), Saitama, Japan. [3]Department of Endocrinology and Metabolism, Graduate School of Medicine, Yokohama City University, Yokohama, Japan. [4]Division of Applied Nutrition, National Institute of Health and Nutrition, Tokyo, Japan. [5]Division of Laboratory Animal Science, Animal Research Center, Tokyo Medical University, Tokyo, Japan. [6]Department of Pathobiochemistry, Faculty of Pharmacy, Meijo University, Nagoya, Japan. [7]Laboratory for Vertebrate Body Plan, Center for Developmental Biology, Institute of Physical and Chemical Research (RIKEN), Kobe, Japan. [8]Genome Science Division, Research Center for Advanced Science and Technology, University of Tokyo, Tokyo, Japan. [9]Institute for Diabetes Care and Research, Asahi Life Foundation, Tokyo, Japan. [10]Department of Cardiovascular Medicine, Graduate School of Medicine, University of Tokyo, Tokyo, Japan.

Glucokinase (Gck) functions as a glucose sensor for insulin secretion, and in mice fed standard chow, haploinsufficiency of β cell–specific Gck (*Gck*$^{+/-}$) causes impaired insulin secretion to glucose, although the animals have a normal β cell mass. When fed a high-fat (HF) diet, wild-type mice showed marked β cell hyperplasia, whereas *Gck*$^{+/-}$ mice demonstrated decreased β cell replication and insufficient β cell hyperplasia despite showing a similar degree of insulin resistance. DNA chip analysis revealed decreased insulin receptor substrate 2 (Irs2) expression in HF diet–fed *Gck*$^{+/-}$ mouse islets compared with wild-type islets. Western blot analyses confirmed upregulated Irs2 expression in the islets of HF diet–fed wild-type mice compared with those fed standard chow and reduced expression in HF diet–fed *Gck*$^{+/-}$ mice compared with those of HF diet–fed wild-type mice. HF diet–fed *Irs2*$^{+/-}$ mice failed to show a sufficient increase in β cell mass, and overexpression of *Irs2* in β cells of HF diet–fed *Gck*$^{+/-}$ mice partially prevented diabetes by increasing β cell mass. These results suggest that Gck and Irs2 are critical requirements for β cell hyperplasia to occur in response to HF diet–induced insulin resistance.

Introduction

Glucokinase (Gck) catalyzes the conversion of glucose into glucose-6-phosphate, and more than 30 years ago Matschinsky and Ellerman proposed that it is critical for glucose sensing (1). Spontaneous inactivating mutations of the *Gck* gene coupled with autosomal-dominant inheritance patterns have been identified in maturity-onset diabetes of the young (MODY) patients (2). These mutations are found in the regions common to the β cell–specific isoform and liver isoform, and both decreased β cell function and impaired glucose uptake by the liver have been suggested to be involved in the pathogenesis of MODY (2). We have previously shown that haploinsufficiency of β cell–specific Gck (*Gck*$^{+/-}$) leads to mild diabetes associated with impaired insulin secretion in response to glucose (3). Gck is now recognized as functioning as a glucose sensor for insulin secretion by pancreatic β cells (4).

Human type 2 diabetes is characterized by 2 major features: peripheral insulin resistance and impaired insulin secretion by pancreatic β cells (5, 6). Blood glucose levels are maintained within the normal range by adaptations of β cell mass and/or function as a compensatory response to insulin resistance. It should be noted that only 15%–20% of obese or severely insulin-resistant subjects become diabetic; the others maintain normoglycemia via β cell compensation (7). Diabetes only develops when insulin secretion by β cells is insufficient to compensate for the insulin resistance. For example, while both insulin receptor substrate 1 (IRS-1) knockout (*Irs1*$^{-/-}$) mice (8, 9) and IRS-2 knockout (*Irs2*$^{-/-}$) mice (10, 11) exhibit similar degrees of insulin resistance, *Irs1*$^{-/-}$ mice have normal glucose tolerance as a result of compensatory β cell hyperplasia, whereas *Irs2*$^{-/-}$ mice develop diabetes because of a lack of β cell hyperplasia in response to insulin resistance. The prevalence of diabetes has increased markedly in both Western countries and Japan, and the increase can be explained by drastic changes in lifestyle, such as a high-fat diet and sedentary lifestyle. Hypertrophic adipocytes produce an excess of hormones and nutrients that have been reported to cause insulin resistance, such as FFAs (12), and secrete less adiponectin, which has been reported to increase insulin sensitivity (13). Tumor necrosis factor α is secreted by macrophages residing within hypertrophied adipose tissue and causes insulin resistance (14). Under insulin-resistant conditions, blood glucose levels are maintained within the normal range by adaptations of β cell mass (hyperplasia) (8, 9). Glucose itself (7); insulin (15); Igfs (16); transcription factors such as insulin promoter factor 1 (Ipf1) and FoxO1 (refs. 17, 18); tyrosine kinase pathways including the insulin receptor (Insr) (19), Igf1 receptor (Igf1r) (19), Irs2 (10, 11), and Akt (20, 21) pathways; the prolactin signaling pathway (22); and Hgf (23) have been reported to be implicated in β cell growth; however, coordinated regulation of β cell mass by these factors under high-fat (HF) diet–induced insulin-resistant conditions has not been fully elucidated. To establish an animal

Nonstandard abbreviations used: CREB, cAMP response element–binding protein; Gck, glucokinase; GSIS, glucose-stimulated insulin secretion; HF, high-fat; Igf1r, Igf1 receptor; Insr, insulin receptor; Ipf1, insulin promoter factor 1; IRS, insulin receptor substrate; βIrs2Tg, β cell Irs2 transgenic (mice); MODY, maturity-onset diabetes of the young; PCNA, proliferating cell nuclear antigen.

Conflict of interest: The authors have declared that no conflict of interest exists.

Citation for this article: *J. Clin. Invest.* 117:246–257 (2007). doi:10.1172/JCI17645.

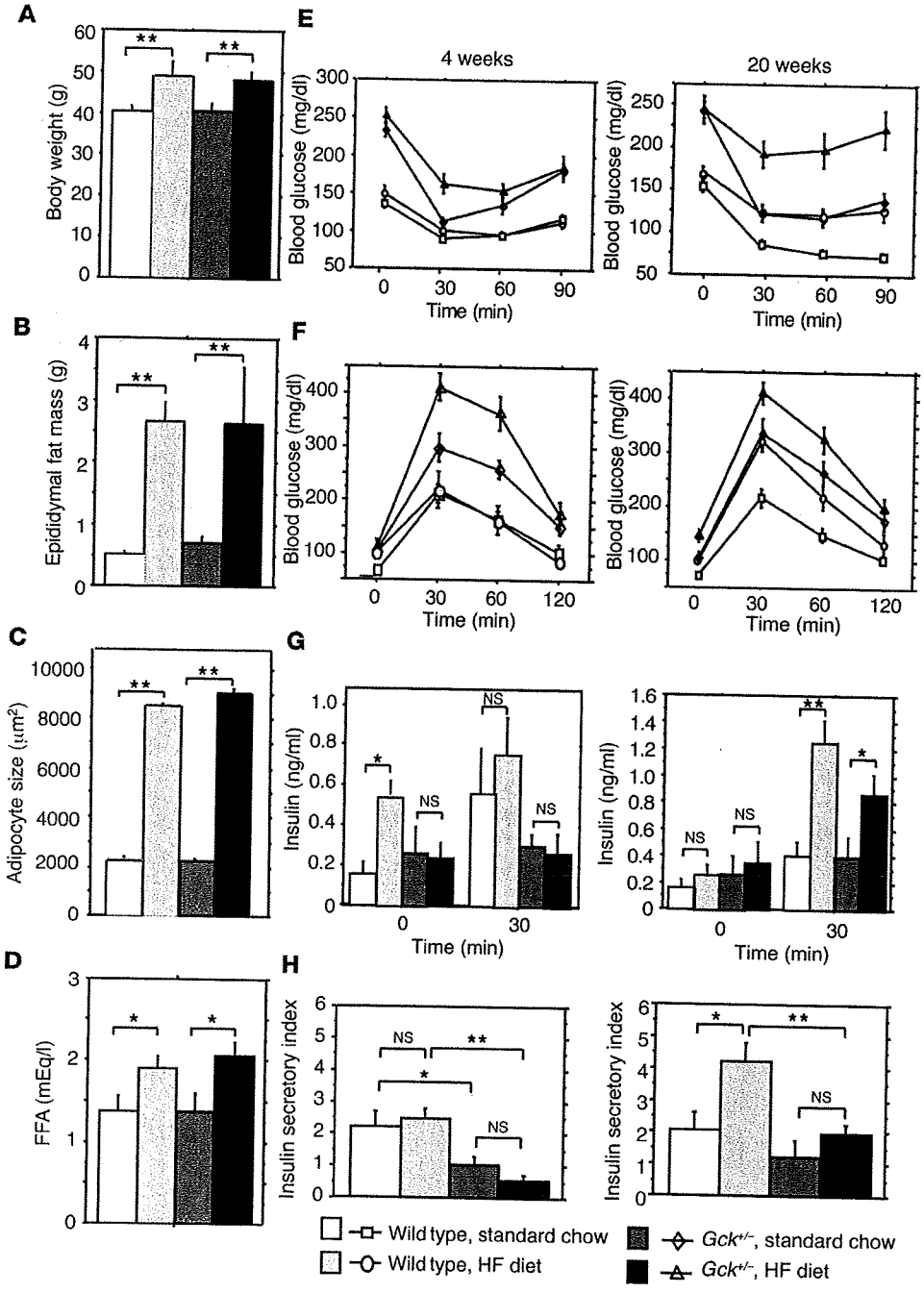

Figure 1
Development of diabetes in *Gck*$^{+/-}$ mice fed HF diet. (**A** and **B**) Body weight (**A**) and total weight of white adipose tissue (epididymal and retroperitoneal fat pads) (**B**) in wild-type and *Gck*$^{+/-}$ mice after 20 weeks on a standard chow or HF diet (n = 17–20). (**C**) Cell size in epididymal white adipose tissue (n = 600–900). (**D**) Serum FFA levels (n = 8–10). (**E**) Insulin tolerance in wild-type and *Gck*$^{+/-}$ mice after 4 weeks (left) and 20 weeks (right) on a standard chow or HF diet. Mice were given free access to food and then intraperitoneally injected with 0.75 mU of human insulin per gram body weight. n = 8 (standard chow–fed wild-type), 9 (HF diet–fed wild-type), 12 (standard chow–fed *Gck*$^{+/-}$), 14 (HF diet–fed *Gck*$^{+/-}$). (**F** and **G**) Glucose tolerance in wild-type and *Gck*$^{+/-}$ mice after 4 and 20 weeks on standard chow or HF diet. (**F**) Plasma glucose levels. (**G**) Serum insulin levels. n = 12 (standard chow–fed wild-type), 13 (HF diet–fed wild-type, standard chow– and HF diet–fed *Gck*$^{+/-}$). (**H**) Insulin secretory index, defined as the ratio of insulin to glucose at 30 minutes after a glucose load. Values represent mean ± SEM. $^{*}P < 0.05$; $^{**}P < 0.01$.

model representative of human type 2 diabetes, we fed wild-type mice and *Gck*$^{+/-}$ mice a HF diet and investigated their glucose homeostasis and β cell mass and function. On the HF diet, wild-type mice showed marked β cell hyperplasia, whereas *Gck*$^{+/-}$ mice demonstrated insufficient β cell hyperplasia despite the presence of a similar degree of insulin resistance. Additionally, expression of *Irs2* was upregulated in the islets of wild-type mice on the HF diet but markedly lower in those of HF diet–fed *Gck*$^{+/-}$ mice, and overexpression of *Irs2* in β cells of HF diet–fed *Gck*$^{+/-}$ mice partially prevented diabetes by increasing β cell mass. Thus, Gck and Irs2 are critical requirements for β cell hyperplasia to occur in response to HF diet–induced insulin resistance.

Results

Early development of diabetes in Gck$^{+/-}$ *mice on a HF diet.* When we fed 8-week-old male wild-type and *Gck*$^{+/-}$ mice a HF diet or standard chow, the 2 genotypes showed similar amounts of body weight gain, adipocyte size, and serum FFA levels that were significantly greater on the HF diet than on standard chow (Figure 1, A–D). After 20 weeks, the glucose-lowering effect of insulin was markedly impaired in both groups on the HF diet compared with those fed standard chow (Figure 1E). After 4 weeks on the HF diet, the wild-type mice maintained normal glucose tolerance as a result of compensatory hyperinsulinemia, whereas the *Gck*$^{+/-}$ mice developed severe diabetes because of a lack of compensatory hyperinsu-

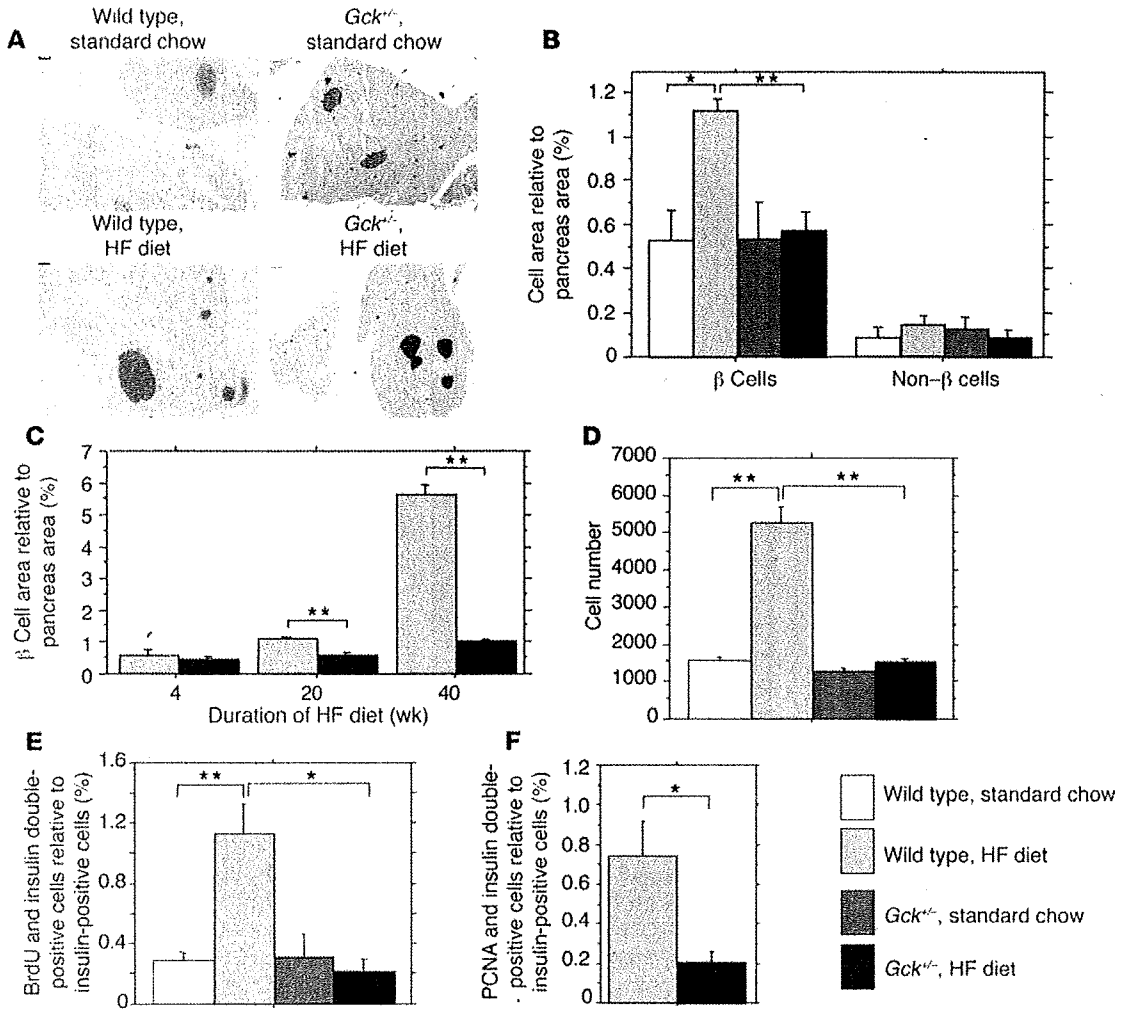

Figure 2

Failure of compensatory β cell hyperplasia in HF diet–fed *Gck*$^{+/-}$ mice caused by decreased β cell replication rate. (**A**) Histologic analysis of pancreatic islets of wild-type and *Gck*$^{+/-}$ mice after 20 weeks on standard chow or HF diet. Sections were double stained with anti-insulin antibody and a cocktail of anti-glucagon, anti-somatostatin, and anti-pancreatic polypeptide antibodies. Representative islets are shown. Red stain, β cells; brown stain, non–β cells. Scale bars: 100 μm. (**B**) Quantitation of β cell and non–β cell mass in wild-type and *Gck*$^{+/-}$ mice after 20 weeks on standard chow or HF diet. Areas of β or non–β cells (α, δ, and pancreatic polypeptide cells) are shown relative to total pancreas area ($n = 4$). (**C**) Changes in β cell mass on HF diet. Shown is β cell area relative to pancreas area ($n = 4$) after 4, 20, and 40 weeks on HF diet. (**D**) Number of cells in wild-type and *Gck*$^{+/-}$ mouse islets after 20 weeks on standard chow or HF diet ($n = 6$). (**E** and **F**) Replication rate of β cells, assayed (**E**) on the basis of BrdU incorporation after 20 weeks on standard chow or HF diet or (**F**) by PCNA staining after 20 weeks on HF diet. Results are shown as ratios of double-positive cells to insulin-positive cells ($n = 4$). Values represent mean ± SEM. $^{*}P < 0.05$; $^{**}P < 0.01$.

linemia (Figure 1, F and G, left panels), despite the similar degrees of obesity and insulin resistance shown by both HF diet–fed groups. Although the wild-type mice on the HF diet developed mild diabetes by 20 weeks, because of the compensatory hyperinsulinemia they never developed severe diabetes (Figure 1, F and G, right panels). After 20 weeks, the insulin-to-glucose ratio 30 minutes after a glucose load (the insulin secretory index) revealed a significantly increased insulin response to glucose in the wild-type mice on the HF diet compared with those fed standard chow, whereas the *Gck*$^{+/-}$ mice on the HF diet had an insulin secretory index similar to that of the *Gck*$^{+/-}$ mice on standard chow (Figure 1H), indicating that no compensatory increase in insulin secretion occurred in the *Gck*$^{+/-}$ mice while on the HF diet.

Failure of compensatory β cell hyperplasia in Gck$^{+/-}$ *mice on the HF diet.* Serum insulin levels are governed by a combination of the insulin secretory capacity of individual β cells and the number of β cells. In this study, we investigated islet mass first. Histologic analysis after 20 weeks on standard chow or HF diet revealed that the HF diet caused islet hyperplasia in the wild-type mice but, surprisingly, no islet hyperplasia in the *Gck*$^{+/-}$ mice (Figure 2A). Quantitative determinations of β cell and non–β cell mass showed that β cell mass increased by 110% in wild-type mice on the HF diet compared with those on standard chow, but that there was no significant increase in *Gck*$^{+/-}$ mice on the HF diet compared with those on standard chow (Figure 2B). After 4, 20, and 40 weeks on the HF diet, the wild-type mice showed 1.2-fold, 2.0-fold, and 10-fold increases, respectively, in